2019

Evaluation of temporal and spatial indicators of regime shifts in shallow lakes

David Adrian Ortiz
Iowa State University

Evaluation of temporal and spatial indicators of regime shifts in shallow lakes

by

David Ortiz

A thesis submitted to the graduate faculty

in partial fulfillment of the requirements for the degree of

MASTER OF SCIENCE

Major: Environmental Science

Program of Study Committee:
Grace Wilkinson, Major Professor
Chris Rehmann
Yuyu Zhou

The student author, whose presentation of the scholarship herein was approved by the program of study committee, is solely responsible for the content of this thesis. The Graduate College will ensure this thesis is globally accessible and will not permit alterations after a degree is conferred.

Iowa State University

Ames, Iowa

2019

DEDICATION

I dedicate my thesis work to my family and supportive friends. I am overwhelmed when I think about the things my parents, Carmen and Guillermo Ortiz, have endured for me to be in a position to pursue my passion of science. My sister, Jennifer Ortiz for being unconditionally understanding with anything I would vent to her in the halls of Bessey. I also dedicate this work to my Sacnistas, my brothers of ΣΛΒ, McNair and Science Bound program faculty, mentors, and peers.

TABLE OF CONTENTS

LIST OF FIGURES

LIST OF TABLES

ACKNOWLEDGMENTS

I would like to thank my primary investigator, Grace Wilkinson, for her unbiased guidance and unconditional support throughout the course of this research. In addition, I would also like to thank my peers in the department and the Wilkinson lab members who have supported me throughout my second adventure at Iowa State University

CHAPTER 1. GENERAL INTRODUCTION

Freshwater harmful algal blooms (HABs) are increasing in frequency, scope, duration, and intensity across the globe. Aquatic ecosystems are negatively affected by HABs, which endanger ecosystem health, human health, and ecosystem services. As such, being able to predict when HABs are going to occur is necessary to prevent or mitigate the negative effects of these events. Freshwater algal blooms are considered a regime shift from clear-water to an algae dominated state. High frequency data simulation and high frequency monitoring of lakes under experimental conditions suggest that statistical early warning indicators (EWIs) such as a rise in autocorrelation (AC) and variance, which can also be measured as the standard deviation (SD) occur before a regime shift. Chapter 1 presents a *post hoc* analysis of temporal EWI detection of the regime shift from a clear state to an algal-dominated state in four shallow, hypereutrophic non-experimental lakes. We evaluated EWIs for four state variables (chlorophyll *a*, phycocyanin, dissolved oxygen, and pH) and two statistical indicators (rises in AC and SD). In addition to our investigation of temporal EWIs in impaired shallow lakes, Chapter 2 explores spatial patterns of state variables prior to, during, and after a regime shift has occurred in a lake. In order to describe these spatial patterns, we sampled state variables weekly across a shallow hypereutrophic lake and examined spatial AC and SD over time.

The four study lakes monitored for Chapter 1 vary in depth, area, shoreline development index, and nutrient concentrations. These ecosystems are in many ways the opposite of the lakes where previous EWI studies have been performed. Despite confounding factors in shallow hypereutrophic lakes such as high and stochastic nutrient loading, a preponderance of primary producers besides phytoplankton, and spatial complexity, we were still able to frequently detect temporal EWIs. We detected 86% of the total possible EWIs signals in our five lake year dataset, with an average of two weeks of warning before bloom conditions appeared. Detection of EWIs was even higher prior to the peak of the bloom, with 96% of the total possible EWIs detected before peak biomass and an average of almost four weeks of warning before bloom climaxes.

Chapter 2 focuses on a shallow, hypereutrophic Swan Lake, we sampled across the entire lake to document patterns of spatial heterogeneity in state variables before, during, and after blooms. There were consistent north-south gradients in the state variable across the lake before and after the bloom and similar variable values across the lake during bloom conditions. We detected rises in spatial AC for all state variables during both bloom events, except phycocyanin which rose ten days before the beginning of the first bloom event. Phycocyanin, dissolved oxygen, and pH rose in spatial SD before bloom conditions and chlorophyll *a* rose during the bloom. However, for the second bloom event chlorophyll *a* rose four weeks in advance and phycocyanin spatial SD rose during bloom conditions. Dissolved oxygen and pH spatial SD did not respond as expected to the second bloom and failing to indicate a regime shift due to contributions from other sources of net ecosystem production besides algae.

In summary, this is the first application of temporal and spatial indicators of a regime shift in shallow, hypereutrophic lakes. These studies provide evidence of the possible multi-pronged approach to detect early warnings to impending blooms using temporal and spatial monitoring. These studies are promising first steps in applying early warning indicator detection in impaired shallow non-experimental lakes. Our studies applied theory derived from high frequency and spatially explicit simulations and verified results from lakes under experimental conditions, by evaluating EWI detection in non-experimental lakes using both space and time monitoring methods. High frequency and spatial monitoring are proving to be efficient, reliable tools in the effort to manage HABs in surface waters.

CHAPTER 2. DETECTING STATISTICAL EARLY WARNING INDICATORS OF ALGAL BLOOMS IN SHALLOW EUTROPHIC LAKES

Modified from a manuscript to be submitted to *Ecosystems*
Authors: David Ortiz[1*], Jason Palmer[2], Grace Wilkinson[1]
[1]Department of Ecology, Evolution, and Organismal Biology, Iowa State University, Ames, Iowa 50010
[2]Iowa Department of Natural Resources, Des Moines, Iowa
*Corresponding Author: daortiz@iastate.edu

Abstract

The regime shift from a clear-water to algae dominated state in freshwater ecosystems often occur abruptly. However, regime shifts are detectable from statistical patterns, which can be interpreted as early warning indicators in advance of the shift. Early warning indicators of the regime shift to an algal-dominated state have been detected using rolling window analysis on simulated data and in lakes under experimental eutrophication through high frequency monitoring. The use of high frequency monitoring for early warning indicators of algal blooms has not been applied and tested outside of lakes under experimental conditions. Non-experimental lakes provide several hurdles that would prevent the detection of early warning indicators such as stochastic nutrient loading, various sources of net ecosystem production, spatial complexity, and larger surface areas relative to the experimental lakes. This study is the first to test the efficacy of high frequency monitoring in non-experimental, shallow, hypereutrophic lakes and in spite of factors that would hinder the early warning detection, we provide evidence of detecting early warnings in advance of a bloom and peak algal biomass. We present early warning detections from five lake years of high frequency chlorophyll *a*, phycocyanin, saturated dissolved oxygen, and pH time series collected from four different impaired shallow lakes, $\leq$ 7m max depth. Warnings were detected on average two weeks prior to chlorophyll *a* and phycocyanin bloom conditions and

almost four weeks before the apex of blooms, using a 15 day rolling window length for our analysis. High frequency monitoring in non-experimental lakes not only provided insight to how impaired lakes bloom, but also provided an important test of efficacy of the application for this increasingly important monitoring tool because of our current global state that is predicted to only experience more eutrophication.

Introduction

Freshwater harmful algal blooms (HABs) are increasing in frequency, scope, duration, and intensity across the globe (Glibert 2017; O'Neil et al. 2012). Aquatic ecosystems are negatively affected by HABs resulting in a loss of biodiversity, anoxic conditions, and the production of toxins by cyanobacteria which dominate many HABs (Landsberg 2002). Human exposure to the toxins produced by cyanobacteria can result in nausea, vomiting, pulmonary consolidation, or liver damage (Chorus et al. 2000; Codd et al. 2005; Corbel et al. 2014). Furthermore, HABs have economic consequences at state and local levels such as reducing revenue from recreational services that lakes provide (Dodds et al. 2009). In short, HABs endanger human health, ecosystem health, and ecosystem services. As such, being able to predict when HABs are going to occur is necessary to prevent or mitigate their effects.

The transition from a clear-water state in lakes to an algal-dominated state, or HAB, is a regime shift. Regime shifts are difficult to predict because of how quickly shifts between states can occur. Despite this, regime shifts are pervasive and have been detected in lake food webs (Carpenter and Brock 2006; Cline et al. 2014; Pace et al. 2013), seagrass beds (Ling et al. 2015; van der Heide et al. 2007), forests (Johnstone et al. 2016; Seidl et al. 2016), coral reefs (Hughes et al. 2018; Wernberg et al. 2016), drylands (D'Odorico et al. 2013; McAllister et al. 2006), and fisheries (Hutchings and Reynolds 2004). A variety of approaches have been used to detect these regime shifts including analysis of spatial patterns over time, (Butitta et al. 2017; Wang and Liu 2005), high frequency monitoring of critical state variables (Carpenter et al. 2014, Gsell et al. 2016, Wilkinson et al. 2018) and a combination of spatial and temporal monitoring (Smith 2018).

Based on theory, regime shifts are preceded by clear statistical patterns in the state variables, termed early warning indicators (EWIs) prior to the critical transition (Carpenter and Brock 2006; Scheffer et al. 2009). These EWIs are a rises in variance, which can also be measured as the standard deviation (SD) or coefficient of variation, and a rise in lag-1 autocorrelation (AC) of a state variable. Rises in SD and AC of state variables are due to critical slowing down of the ecosystem (Carpenter and Brock 2006; Dakos et al. 2011; Dakos et al. 2012; Dakos et al. 2015). The SD and AC of state variables over time is calculated using a rolling window analysis on high frequency data. Detecting EWIs using temporal data is difficult due to compounding factors including the frequency of data collection, the start of data collection in relation to the regime shift, data collection methods, and various statistical approaches used to identify EWIs (Gsell et al. 2016).

The ability to detect EWIs prior to HABs has been demonstrated in experimental whole-lake manipulations where cyanobacteria blooms are induced with nutrient additions to oligotrophic ecosystems (Butitta et al. 2017; Carpenter et al. 2011; Pace et al. 2016; Wilkinson et al. 2018). While these experiments provided important proof-of-concept that EWIs could be detected prior to a regime shift, questions remain regarding the effectiveness of EWIs for predicting HABs in non-experimental lakes. These experiments purposefully induced regime shifts with regular additions of known quantities of nitrogen and phosphorus. However, in non-experimental ecosystems, nutrient inputs are episodic in time and space, which interfere with EWI detection (Carpenter and Brock 2006). What's more, the experimental lakes were oligotrophic prior to the nutrient additions, and likely had a higher resilience at the beginning of the experiment than a non-experimental, nutrient-rich lake. A higher initial resilience could increase the likelihood of observing EWIs prior to the critical transition because it would lengthen the period leading up to the regime shift.

In order to evaluate if EWIs are detectable in non-experimental lakes, we monitored four hypereutrophic lakes with extensive histories of HABs. We used the similar high frequency HAB monitoring and EWI detection techniques as described in the experimental lake studies (Wilkinson et al. 2018) to determine the detectability of EWIs in lakes under non-experimental conditions. Specifically, we used the gradient of lake conditions to test whether there were consistent rises in SD and AC prior to the onset of bloom conditions and peak algal biomass in lakes. From this *post hoc* analysis, we make recommendations for future HAB monitoring for the detection of EWIs.

Methods

We collected high frequency time series during the growing seasons of 2014, 2015, and 2018 in four shallow lakes that experience frequent algal blooms for a total of five lake years of data. The study lakes spanned a range of surface area and depths. All the lakes were hypereutrophic (Carlson 1977), largely due to high degrees of agricultural land use in the watersheds (Arbuckle and Downing 2001) (Table 1.1). The lakes in our study were all also on the Clean Water Act 303(d) list of impaired waters at the time of sampling for excessive algal growth or bacterial impairment.

The high frequency time series were collected using YSI EXO2 and YSI EXO3 multiparameter sondes (Yellow Springs Instrument, Yellow Springs, OH) equipped with sensors for Total Algae, which includes chlorophyll *a* and phycocyanin, dissolved oxygen saturation (DO), pH, and temperature. DO is a potential state variable to monitor for the regime shift to algal dominance as it responds to the increase in photosynthesis (Batt et al. 2013; Odum 1956; Sirota et al. 2013). Another variable that responds to primary production is pH. As dissolved carbon dioxide is removed from the water column by photosynthesis, which decreases the amount of carbonic acid, thereby causing pH to increase. Increases in both DO and pH indicate increasing of phytoplankton biomass. The sondes were deployed approximately 0.5m below the surface at the historical deep site in each lake during the ice-free period. The sensors were calibrated every two weeks from 2014-2015 and regularly in 2018 when indicated by the KorDSS software with functionality to detect instrument drift during deployment. The length of the time series ranged from 91 to 153 days of continuous high frequency (15 min) data collection (Table 1.2).

Synoptic water quality samples, which included total nitrogen and phosphorus and the algal pigments, chlorophyll *a* and phycocyanin, were taken regularly during the sonde deployment periods (Table 1.1). Total nitrogen was measured as the sum of total Kjeldahl nitrogen (US EPA 1993, method 351.2 v2) and nitrate + nitrite measured using the cadmium reduction method (US EPA 1993, method 4500-NO_3-F). Total phosphorus was measured using the ascorbic acid method (US EPA 1993, method 365.1 v2) while chlorophyll *a* was measured via acetone extraction (US EPA 1993, method 10200-H) and phycocyanin was extracted in a sodium phosphate buffer (Sadra et al. 1999). The algal pigment data were used to verify the calibrated high frequency sonde measurements.

There is not a standard definition for what constitutes an algal bloom state versus a non-bloom state in lakes. Studies that have provided a definition based on a threshold biomass of algae have used long-term data with robust observations of the water body in a non-bloom state (Smayda 1997; Wilkinson et al. 2018). Using the relative changes in algal concentrations over time for each lake year is an alternative method for defining a blooming period. For this study, we define a bloom as beginning when pigment concentrations (chlorophyll *a* or phycocyanin) double over the course of five consecutive days or less. We also define the peak of the bloom as the peak concentration of algal biomass based on the peak concentration of chlorophyll *a*. This method provides distinct pre-bloom, blooming, and post-bloom periods for ecosystems without historic pigment data. Additionally, by not defining a threshold of biomass, the definition of a bloom we are using based on biomass dynamics is applicable to a variety of waterbodies at various trophic states (Carlson 1977).

Using our bloom definition based on algal biomass dynamics, we defined three key periods: 1) the pre-bloom period when biomass was low with little day-to-day change, 2) the bloom period when pigment concentrations were rapidly increasing, and 3) peak biomass when the bloom was at its apex and either remained at high biomass or began to diminish. The last day of the pre-bloom period is also the last day for detecting “true” EWIs before bloom conditions. The period prior to peak biomass marks the onset of the bloom, with EWIs prior to this point signifying early notice of the peak instead of the onset of a bloom. Continuing to search for EWIs after bloom conditions occur still provides insight of bloom conditions may worsen and provides a longer period for intervention.

The evaluation of EWIs performance was *post hoc*, using a rolling window analysis of daily averages of the state variables. While there are many candidate EWI statistics (Dakos et al 2012), in this study we examined lag-1 AC and SD as these statistics have successfully detected the regime shift in question in experimental manipulations (Batt et al. 2013, Pace et al. 2017, Wilkinson et al. 2018). We considered an EWI to begin when there were three consecutive days of increase in the rolling window statistic and began to count the warning period from that first day of increase. We selected the three day minimum as a balance between decreasing false positives and being able to detect an EWI signal. We evaluated the rolling window time series of SD and AC prior to both the pre-bloom conditions and the peak biomass for "true" early warnings and EWIs that occurred prior to the apex of the bloom. For assessing EWIs in pH and DO, we referenced the chlorophyll *a*-defined bloom stages because chlorophyll *a* is representative of the entire phytoplankton community and not just cyanobacteria, which may or may not dominate the bloom. However, if there was not a bloom based on the chlorophyll *a*, we used the same bloom definition with the phycocyanin time series and applied those bloom periods to the DO and pH time series.

A rolling window analysis uses a predetermined range of days of a state parameter time series to calculate a summary statistics (AC and SD). The rolling window moves forward one time step, retaining the same range of days, partially overlapping the range of the previous time step. Rolling window analysis of AC and SD of the chlorophyll *a*, phycocyanin, DO and pH time series, and sensitivity analyses were done in R (version 1.1.456; R Core Development Team 2018) with the "earlywarning" package (Dakos et al. 2012). Rolling window length sensitivity was tested for a range of 10 – 21 days and we present the results for a 15 day window length analysis of the entire dataset (see Appendix for the 10-day and 21-day results). The window length used in this study is shorter than previous EWI studies (Carpenter et al. 2011; Pace et al. 2017; Wilkinson et al. 2018) because of unknown high frequency bloom dynamics in shallow hypereutrophic lakes due to the episodic nutrient loading. In addition, the 15 day window length is a compromise between EWI detection sensitivity and decreasing short term variability unrelated to the impending regime shift.. Selecting a longer window length would have introduced new issues for detecting EWIs in our dataset. A longer window length would capture all pre-bloom, bloom and possibly post bloom dynamics all within several window time steps, making the statistics difficult to interpret. In addition, a longer window length would miss bloom dynamics that occurred early in the time series, sometimes occurring before 15 days of sonde deployment.

As for what constitutes an interpretable rise of rolling window statistics as an EWI the definition is vague and open for interpretation. There are no consistent literature indicating thresholds for AC and SD rolling window statistics nor rates of change. For this study, we used an operational definition of three consecutive days of an increase in the rolling window statistics before the end of pre-bloom condition and the peak biomass were identified as EWIs. For our analysis, we also considered there to be only one EWI for each variable (chlorophyll *a*, phycocyanin, DO, and pH) and one EWI for each statistic (AC and SD) before either bloom conditions or peak biomass, for eight possible EWIs.

Results

All five lake years experienced blooms based on both the chlorophyll *a* and phycocyanin time series (Figures 1.1-1.5). Chlorophyll *a* referenced bloom conditions occurred at similar times to phycocyanin bloom, ranging from the same day to two days after with the exception of Green Valley Lake 2015. Phycocyanin-based bloom conditions followed chlorophyll *a* bloom conditions up to 31 days after. Swan Lake 2018 phycocyanin bloom peak occurred twelve days before the chlorophyll *a* apex. South Twin 2018 and Green Valley 2014 chlorophyll *a* apex respectively occurred on the same day or a day in advance of phycocyanin. Black Hawk Lake 2015 and Green Valley 2015 had their chlorophyll *a* peaks 16 and 69 days, respectively, before phycocyanin apexes. In two of the lake years, Blackhawk 2015 and Green Valley 2014 (Figures 1.1 & 1.2), two separate bloom events occurred, in both the chlorophyll and phycocyanin time series. Black Hawk Lake 2015 and Green Valley 2015 had their second chlorophylls *a* bloom events occur a mean of four days and peaks a mean of 18 days prior to their phycocyanin counterpart blooms (Figure 1.5). The largest chlorophyll-based bloom was in Blackhawk 2015 with a maximum concentration of 169 $\mu g\ L^{-1}$. This bloom was likely not dominated by cyanobacteria as it coincided with one of the lowest phycocyanin beak biomasses of 16 $\mu g\ L^{-1}$ (Figure 1.1). Green Valley in 2015 displayed the opposite pattern, with the highest phycocyanin biomass peak of all the lakes at 70.2 $\mu g\ L^{-1}$and a lower peak chlorophyll *a* concentration of 29.2 $\mu g\ L^{-1}$ (Table 1.2; Figure 1.3). The bloom in South Twin Lake was already occurring when sonde measurements began, with peak chlorophyll concentrations occurring only after 21 (Figure 1.4). The time series of DO and pH rose with pigment concentrations in Blackhawk 2015, Green Valley Lake 2014, and Green Valley Lake 2015 (Figures 1.1-1.3). However, the peak concentrations of DO and pH values occurred after the peak biomass in South Twin Lake 2018 and Swan Lake 2018 (Figures 1.4 & 1.5).

All five lake years had rises in the AC and SD rolling window statistics for many of the state variables, which are interpreted as EWIs (Table 1.3). The detection of EWI signals varied among lake years, state variables, rolling window statistics (AC and SD), and for second bloom events (Table 1.3; Figure 1.6). Rolling window length affects the dynamics of AC and SD rolling window statistics. Decreasing the window length from 15 to 10 days, resulted in 30% more rises in AC and SD, indicating that the EWI detection is sensitive to rolling window length and too short of a window leads to false warnings (Fig. S1.1). Increasing the window length to 21 days from 15 days, decreased the warning period prior to blooms and peak biomass, reducing the total number of EWIs by 25% across all lake years.

South Twin lost all EWIs when using a rolling window length of 21 days and chlorophyll *a* EWIs were lost in Green Valley 2014 and 2015 (Fig. S1.2 & S1.3).

Blackhawk Lake 2015 had the longest warning period in our five lake year dataset for both pre-bloom and peak biomass for all state variables in both rolling window statistics (Figure 1.6). Blackhawk Lake 2015 also had the longest total time series (155 days) and the longest pre-bloom time series length (52 days). Blackhawk Lake 2015 pigment rolling window time series of AC and SD EWIs had a mean of 23 days of warning prior to the onset of the first bloom (Figure 1.7). The earliest EWIs detected in Blackhawk Lake 2015 began 77 days in advance of the phycocyanin peak biomass (Figure 1.6). The pH- and DO-based EWIs were detected prior to the onset of the bloom and before peak biomass, but were detected approximately 10 days after the pigment-based EWIs.

Green Valley Lake 2014 and 2015 had longer warning periods in the phycocyanin time series than in other state variable EWIs (Figure 1.6). Green Valley 2014 did not produce any EWIs prior to the first blooms or peak biomass for chlorophyll *a* and phycocyanin because of bloom conditions occurring within 15 days of the sonde being deployed (Figure 1.2). Similarly, Green Valley Lake 2015 only had warnings before peak chlorophyll *a* biomass for pH- and DO- based EWIs, because of early bloom dynamics occurring within 15 or less days after the sonde was deployed (Figure 1.3). Green Valley 2014 experienced a second bloom in both pigments and this event was captured by EWIs for both AC and SD in the state variables, with warning period lengths on par with the overall dataset mean warning lengths (Figure 1.7).

South Twin Lake has the shortest time series length (99 days) and no pre-bloom stage. Therefore, by definition, no pre-bloom EWIs were detected. The warning period lengths prior to the peak biomass was the shortest of all of the lake years (Fig. 1.6), producing warnings of 4 days for both pigment-based and pH EWIs, and 7 days for DO-based EWIs (Figure 1.4). Similar to South Twin 2018, there were no pre-bloom EWIs detected in Swan Lake 2018 for any state variables (Figure 1.5). The sonde deployment in Swan Lake 2018 was unable to capture pre-bloom EWIs with the short pre-bloom period length of 15 days. Warnings were detected for all state variables immediately after bloom conditions occurred in Swan Lake 2018, and were detected on average 22 days before peak biomass (Figure 1.5).

Across the entire five lake year dataset, detection of AC- and SD- based EWIs were comparable, each statistic only failing to produce one warning (Figure 1.6). Of the total possible 28 true EWIs, in which rolling window AC and SD were calculated before bloom conditions, 86% were detected. Additionally, 96% of total possible of both AC and SD EWIs before peak bloom biomass in the entire five lake year dataset. Mean warning periods for AC and SD were also similar, 24 days and 22 days, respectively for both bloom events. Longest warning periods were different for each statistic, AC had the longest warning period with 77 days and SD had 65 days (Figure 1.6; Table 1.3). The shortest warning period lengths were four days and three days, AC and SD respectively. Phycocyanin-based EWIs consistently had the longest warning period with a mean of 25 days for both bloom events and both pre-bloom and peak biomass (Figure 1.6; Table 1.3). Chlorophyll *a* had the shortest mean warning length of 20 days, pH had a mean warning length of 23 days, and DO had a mean warning length of 24 days for all lake years and both statistics (Table 1.3). Lakes with longer time series, Blackhawk Lake 2015 and Green Valley Lake 2015, had longer mean warning periods than the lakes with shorter time series, Green Valley 2014, South Twin 2018, and Swan Lake 2018 (Figure 1.7).

Discussion

This study provides evidence that EWIs are detectable prior to the onset and peak of HABs in nutrient-rich, shallow lakes. Three of the seven bloom events recorded had a rise in SD or AC in at least one state variable prior to the onset of the bloom. The rises in AC and SD were detected, on average, approximately two weeks prior to the onset of the bloom in these lakes, providing ample warning for management and intervention. When considering the apex of the bloom, all five lake years had EWIs prior to the peak biomass with a mean warning period of almost four weeks. While these are not truly early warnings in the sense that the bloom has already begun, the EWI signal prior to the peak still provides information and warning that can be used to intervene or mitigate the effects of the bloom.

Our study lakes vary in depth, area, shoreline development index, and nutrient concentrations. Our study lakes represent the other extreme of trophic states when compared to ecosystems of previous HAB EWI studies have been conducted (e.g. Pace et al. 2017; Wilkinson et al. 2018). Our study represents a subset of freshwater lakes, and the results are pertinent to limnologists as lakes across the globe are experiencing eutrophication. Despite all of the confounding and unknowable effects that hypereutrophic and shallow lake possess, our study was still able to detect a high percentage of total EWIs.

Three of our lakes, Green Valley 2014, South Twin 2018, and Swan 2018 lacked the possibility of detecting pre-bloom EWIs due to tardy sonde deployment, relative to the early bloom conditions in these ecosystems. Lakes that produced the timeliest EWIs had sonde deployments longer than 127 consecutive days. Our results demonstrate that a monitoring program designed to detect EWIs of HABs will require extending lake monitoring periods.

Typically, lake monitoring occurs during ice-off periods, which does not lend itself to fully capturing all dynamics in aquatic systems. There is a large proportion of the yearly metabolic activity occurring under ice (Hampton et al. 2017; Pernica et al. 2017), which could improve EWI monitoring in shallow hypereutrophic systems. The time series for our studies began well after ice-free conditions, which generally occur around DOY 90. Sondes at Green Valley 2014 and South Twin Lake 2018 were deployed on DOY 152 and Swan Lake 2018 on DOY 138, deploying sondes at these lakes well after ice-off caused time series to begin during bloom conditions or within 15 days of bloom conditions. A long time period of pre-bloom conditions relative to the rolling window length is necessary to capture the dynamics in the EWI rolling window analysis. Given these constraints, happenstance high frequency data collection is unlikely to be suitable for EWI detection (Gsell et al. 2016).

Several other variables may have affected the efficacy of the EWI detection in our study lakes. In our study, we deployed the sondes about 0.5m from the surface. However, even at this depth, phytoplankton biomass may have been over or under represented particularly scum-forming blooms. Cyanobacteria can regulate their location in the water column, meaning that they can migrate above or below the sensors, influencing the total biomass estimate based on the pigment concentrations (Cui et al. 2016; Klemer et al. 1996). These lakes are also spatially complex and were only sampled at their historic deep points. Positioning sondes in identified algal hotspots that consistently bloom first or for the longest period may yield more robust EWI detection (Alexander and Imberger 2009; Dokulil and Teubner 2000). The use of DO and pH as state variables also makes the assumption that phytoplankton are the only significant contributors to net ecosystem production. However, some of our lakes contained dense macrophyte communities and possibly benthic algae, which could be a major driver of DO and pH dynamics. As such, relying solely on these secondary proxies of primary production may not be completely trustworthy to represent only bloom dynamics (Carpenter and Lodge 1986).

Our study reinforces the possibility of using high frequency monitoring for EWIs as a lake management strategy. We were able to detect EWIs on average of two weeks to prior bloom conditions and up to ten weeks before the bloom apex in hypereutrophic lakes. These wide and timely warning periods would allow lake managers to communicate with the surrounding communities of the impending hazards such as potential cyanotoxin concentrations in the upcoming weeks. If resources are available, these warning periods can also allow lake management to mitigate the bloom’s potential impact on the ecosystem using techniques such as aerators, algaecides, and harvesting (Carmichael et al. 2000; Lilndenschmidt 1999; Ma and Liu 2002). Continued work on our study lakes is be required to better understand how to best monitor taking into consideration of each lakes’ unique characteristics enabling a more robust conclusions about bloom dynamics and how they relate to EWIs.

This study not only addressed the promising potential use of high frequency monitoring of EWIs to warn of oncoming blooms and bloom peaks, but we also identified new knowledge gaps. Are there lakes that lend themselves to EWIs detection more readily than others? How early do sondes need to be deployed in the ice-off period or do we need to monitor year round? Can high frequency monitoring be enhanced by supplementing with spatial data or can spatial data predict blooms better? What is the reliability of pH and DO when macrophytes and benthic algae are present? While we were able to begin addressing many of these questions (e.g. the reliability of pH and DO as state variables and the monitoring period needed), these questions need to be further addressed before EWI detection can be recommended as a tool for lake management. The use of high frequency monitoring in lakes under non-experimental conditions is an ecosystem science frontier and a corner stone in understanding blooming hypereutrophic systems. This study expands our understanding of regime shifts in lakes, by moving into the realm of testing the efficacy of EWI detection in different aquatic systems. Our study applied theory in lakes under non-experimental conditions and produced results that are in support of previous simulated and experimental conclusions of regime shift detection. High frequency monitoring is proving itself an efficient and reliable tool in the effort to understand and manage our heavily impaired waterbodies.

Acknowledgments

We would like to thank Ryan Wagner, Ellen Albright, and Tyler Butts for assistance with data collection for instrument deployment and collection. We would also like to thank Rachel Fleck for water sample processing guidance. Funding provided by the Center for Global and Regional Environmental Research, the Iowa State University Graduate Minority Assistantship Program, and the Iowa State University Graduate Research Assistantship Match Program.

References

Alexander, R., and J. Imberger. 2009. Spatial distribution of motile phytoplankton in a stratified reservoir: the physical controls on patch formation. Journal of Plankton Research **31:** 101-118.

Arbuckle, K. E., and J. A. Downing. 2001. The influence of watershed land use on lake N : P in a predominantly agricultural landscape. Limnology and Oceanography **46:** 970-975.

Batt, R. D., S. R. Carpenter, J. J. Cole, M. L. Pace, and R. A. Johnson. 2013. Changes in ecosystem resilience detected in automated measures of ecosystem metabolism during a whole-lake manipulation. Proceedings of the National Academy of Sciences of the United States of America **110:** 17398-17403.

Butitta, V. L., S. R. Carpenter, L. C. Loken, M. L. Pace, and E. H. Stanley. 2017. Spatial early warning signals in a lake manipulation. Ecosphere **8**. DOI: 10.1002/ecs2.1941

Carmichael, W. W., C. Drapeau, and D. M. Anderson. 2000. Harvesting of Aphanizomenon flos-aquae Ralfs ex Born. & Flah. var. flos-aquae (Cyanobacteria) from Klamath Lake for human dietary use. Journal of Applied Phycology **12:** 585-595.

Carpenter, S. R., and W. A. Brock. 2006. Rising variance: a leading indicator of ecological transition. Ecology Letters **9:** 308-315.

Carpenter, S. R. and others 2011. Early Warnings of Regime Shifts: A Whole-Ecosystem Experiment. Science **332:** 1079-1082.

Carpenter, S. R., and D. M. Lodge. 1986. Effects Of Submersed Macrophytes On Ecosystem Processes. Aquatic Botany **26:** 341-370.

Chorus, I., I. R. Falconer, H. J. Salas, and J. Bartram. 2000. Health risks caused by freshwater cyanobacteria in recreational waters. Journal of Toxicology and Environmental Health-Part B-Critical Reviews **3:** 323-347.

Cline, T. J. and others 2014. Early warnings of regime shifts: evaluation of spatial indicators from a whole-ecosystem experiment. Ecosphere **5**. DOI: 10.1890/es13-00398.1

Codd, G. A., L. F. Morrison, and J. S. Metcalf. 2005. Cyanobacterial toxins: risk management for health protection. Toxicology and Applied Pharmacology **203:** 264-272.

Corbel, S., C. Mougin, and N. Bouaicha. 2014. Cyanobacterial toxins: Modes of actions, fate in aquatic and soil ecosystems, phytotoxicity and bioaccumulation in agricultural crops. Chemosphere **96:** 1-15.

Cui, Y. J. and others 2016. Diel migration of Microcystis during an algal bloom event in the Three Gorges Reservoir, China. Environmental Earth Sciences **75**. DOI: 10.1007/s12665-015-5124-x

D'Odorico, P., A. Bhattachan, K. F. Davis, S. Ravi, and C. W. Runyan. 2013. Global desertification: Drivers and feedbacks. Advances in Water Resources **51:** 326-344.

Dakos, V. and others 2012. Methods for Detecting Early Warnings of Critical Transitions in Time Series Illustrated Using Simulated Ecological Data. Plos One **7**. DOI: 10.1371/journal.pone.0041010

Dakos, V., S. R. Carpenter, E. H. van Nes, and M. Scheffer. 2015. Resilience indicators: prospects and limitations for early warnings of regime shifts. Philosophical Transactions of the Royal Society B-Biological Sciences **370**. DOI: 10.1098/rstb.2013.0263

Dakos, V., S. Kefi, M. Rietkerk, E. H. van Nes, and M. Scheffer. 2011. Slowing Down in Spatially Patterned Ecosystems at the Brink of Collapse. American Naturalist **177:** E153-E166.

Dodds, W. K. and others 2009. Eutrophication of US Freshwaters: Analysis of Potential Economic Damages. Environmental Science & Technology **43:** 12-19.

Dokulil, M. T., and K. Teubner. 2000. Cyanobacterial dominance in lakes. Hydrobiologia **438:** 1-12.

Glibert, P. M. 2017. Eutrophication, harmful algae and biodiversity - Challenging paradigms in a world of complex nutrient changes. Marine pollution bulletin **124:** 591-606.

Hampton, S. E. and others 2017. Ecology under lake ice. Ecology Letters **20:** 98-111.

Hughes, T. P. and others 2018. Spatial and temporal patterns of mass bleaching of corals in the Anthropocene. Science **359:** 80-83.

Hutchings, J. A., and J. D. Reynolds. 2004. Marine fish population collapses: Consequences for recovery and extinction risk. Bioscience **54:** 297-309.

Johnstone, J. F. and others 2016. Changing disturbance regimes, ecological memory, and forest resilience. Frontiers in Ecology and the Environment **14:** 369-378.

Klemer, A. R., J. J. Cullen, M. T. Mageau, K. M. Hanson, and R. A. Sundell. 1996. Cyanobacterial buoyancy regulation: The paradoxical roles of carbon. Journal of Phycology **32:** 47-53.

Landsberg, J. H. 2002. The effects of harmful algal blooms on aquatic organisms. Reviews in Fisheries Science **10:** 113-390.

Lilndenschmidt, K. E. 1999. Controlling the growth of Microcystis using surged artificial aeration. International Review of Hydrobiology **84:** 243-254.

Ling, S. D. and others 2015. Global regime shift dynamics of catastrophic sea urchin overgrazing. Philosophical Transactions of the Royal Society B-Biological Sciences **370**. DOI: 10.1098/rstb.2013.0269

Ma, J., and W. Liu. 2002. Effectiveness and mechanism of potassium ferrate(VI) preoxidation for algae removal by coagulation. Water Research **36:** 871-878.

McAllister, R. R. J., I. J. Gordon, M. A. Janssen, and N. Abel. 2006. Pastoralists' responses to variation of rangeland resources in time and space. Ecological Applications **16:** 572-583.

O'Neil, J. M., T. W. Davis, M. A. Burford, and C. J. Gobler. 2012. The rise of harmful cyanobacteria blooms: The potential roles of eutrophication and climate change. Harmful Algae **14:** 313-334.

Odum, H. T. 1956. Primary Production In Flowing Waters. Limnology and Oceanography **1:** 102-117.

Pace, M. L. and others 2017. Reversal of a cyanobacterial bloom in response to early warnings. Proceedings of the National Academy of Sciences of the United States of America **114:** 352-357.

Pace, M. L., S. R. Carpenter, R. A. Johnson, and J. T. Kurtzweil. 2013. Zooplankton provide early warnings of a regime shift in a whole lake manipulation. Limnology and Oceanography **58:** 525-532.

Pernica, P., R. L. North, and H. M. Baulch. 2017. In the cold light of day: the potential importance of under-ice convective mixed layers to primary producers. Inland Waters **7:** 138-150.

Sadra, A., M. G. Pillai, and G.A. Ravishankar. 1999. Phycocyanin from Spirulina sp: influence of processing of biomass on phycocyanin yield, analysis of efficacy of extraction methods and stability studies on phycocyanin. Process Biogeochemistry 34: 795-801.

Scheffer, M. and others 2009. Early-warning signals for critical transitions. Nature **461:** 53-59.

Seidl, R., T. A. Spies, D. L. Peterson, S. L. Stephens, and J. A. Hicke. 2016. Searching for resilience: addressing the impacts of changing disturbance regimes on forest ecosystem services. Journal of Applied Ecology **53:** 120-129.

Sirota, J., B. Baiser, N. J. Gotelli, and A. M. Ellison. 2013. Organic-matter loading determines regime shifts and alternative states in an aquatic ecosystem. Proceedings of the National Academy of Sciences of the United States of America **110:** 7742-7747.

Smayda, T. J. 1997. What is a bloom? A commentary. Limnology and Oceanography **42:** 1132-1136.

Smith, C.D., 2018, Temporal and spatial monitoring of cyanobacterial blooms at Willow Creek Reservoir, north-central Oregon: U.S. Geological Survey Scientific Investigations Report 2018–5083, 26 p. DOI: 10.3133/sir20185083

United States Environmental Protection Agency. 1993. Determination of Nitrate-Nitrite by Automated Colorimetry. Method 353.2 Revision 2.0.

United States Environmental Protection Agency. 1993. Determination of Phosphorus by Semi-Automated Colorimetry. Method 365.1 Revision 2.0.

United States Environmental Protection Agency. 1993. Determination of Total Kjeldahl Nitrogen by Semi-Automated Colorimetry. Method 351.2 Revision 2.0.

van der Heide, T., E. H. van Nes, G. W. Geerling, A. J. P. Smolders, T. J. Bouma, and M. M. van Katwijk. 2007. Positive feedbacks in seagrass ecosystems: Implications for success in conservation and restoration. Ecosystems **10:** 1311-1322.

Wang, X. J., and R. M. Liu. 2005. Spatial analysis and eutrophication assessment for chlorophyll a in Taihu Lake. Environmental Monitoring and Assessment **101:** 167-174.

Wernberg, T. and others 2016. Climate-driven regime shift of a temperate marine ecosystem. Science **353:** 169-172.

Wilkinson, G. M. and others 2018. Early warning signals precede cyanobacterial blooms in multiple whole-lake experiments. Ecological Monographs **88:** 188-203.

Tables

Table 2.1 Summary of water quality parameters and lake characteristics for each lake year including mean total nitrogen (TN), and mean total phosphorous (TP). Agricultural land use in their respective HUC12 watershed.

Lake	**Year**	**Latitude**	**Longitude**	**Surface Area (ha)**	**Max Depth (m)**	**% Watershed Ag**	**Trophic State**	**TN (mg/L)**	**TP (mg/L)**
Blackhawk	2015	42.297	-95.016	295	4.6	74.8	hypereutrophic	4.30	0.24
Green Valley	2014	41.1032	-94.387	136.8	7	86.1	hypereutrophic	2.27	0.18
	2015						hypereutrophic	2.56	0.27
South Twin	2018	42.4627	-94.653	242.8	1.6	83.5	hypereutrophic	2.65	0.19
Swan	2018	42.0396	-94.845	40.5	3	92.3	hypereutrophic	2.57	0.28

Table 2.2 The length of the high frequency time series and the mean and range of values of the four state variables.

			Chlorophyll *a* (µg/L)		Phycocyanin (µg/L)		pH		Dissolved Oxygen (% saturation)	
Lake	Year	Time series length	Mean	Range	Mean	Range	Mean	Range	Mean	Range
Blackhawk	2015	153	45.7	0.1 - 169.1	3.8	0.2 - 14.0	8.5	7.7 - 9.2	115	43.2 - 195.7
Green Valley	2014	99	13.6	1.9 - 51.2	7.2	0.4 - 28.9	8.3	7.5 - 9.6	82.6	11.3 - 211.4
Green Valley	2015	151	7.9	0.9 - 29.2	13.8	0.4 - 70.2	9.2	7.9 - 10.3	109.8	61.0 - 314.8
South Twin Lake	2018	99	19	6.6 - 92.8	7.3	0.2 - 20.8	8.8	8.0 - 9.3	107.2	62.7 - 206.1

Table 2.3 A summary of the number of days of early warning indicators (EWI) were detected prior to the beginning of bloom conditions and before peak biomass. The emdash (—) indicates when an EWI was not detected prior to the onset of bloom conditions or peak biomass. Asterisks (*) indicate that the sonde deployment was too late to detect an EWI as the bloom began within 15 days of the first measurement. Lakes where there was no 2nd bloom in that lake year and no possible EWI detection, are indicated with "na".

		1st Bloom				2nd Bloom			
		Pre-bloom EWI		EWI prior to Peak Biomass		Pre-bloom EWI		EWI prior to Peak Biomass	
	LAKE YEAR	**AC**	**SD**	**AC**	**SD**	**AC**	**SD**	**AR**	**SD**
CHL	*Black Hawk 2015*	34	13	61	40	18	-	29	8
	Green Valley 2014	*	*	*	*	8	10	17	19
	Green Valley 2015	*	*	—	10	na	na	na	na
	South Twin 2018	*	*	6	4	na	na	na	na
	Swan 2018	*	*	27	27	na	na	na	na
PHYCO	*Black Hawk 2015*	33	13	77	57	-	-	29	29
	Green Valley 2014	*	*	*	*	14	8	32	26
	Green Valley 2015	9	8	65	56	na	na	na	na
	South Twin 2018	*	*	4	—	na	na	na	na
	Swan 2018	—	—	13	12	na	na	na	na
pH	*Black Hawk 2015*	28	27	55	54	21	17	32	28
	Green Valley 2014	*	*	*	*	8	10	17	19
	Green Valley 2015	*	*	5	9	na	na	na	na
	South Twin 2018	*	*	4	3	na	na	na	na
	Swan 2018	*	*	24	24	na	na	na	na
DO	*Black Hawk 2015*	38	38	65	65	21	17	32	28
	Green Valley 2014	*	*	*	*	8	10	17	19
	Green Valley 2015	*	*	5	10	na	na	na	na
	South Twin 2018	*	*	7	6	na	na	na	na
	Swan 2018	*	*	21	27	na	na	na	na

Figures

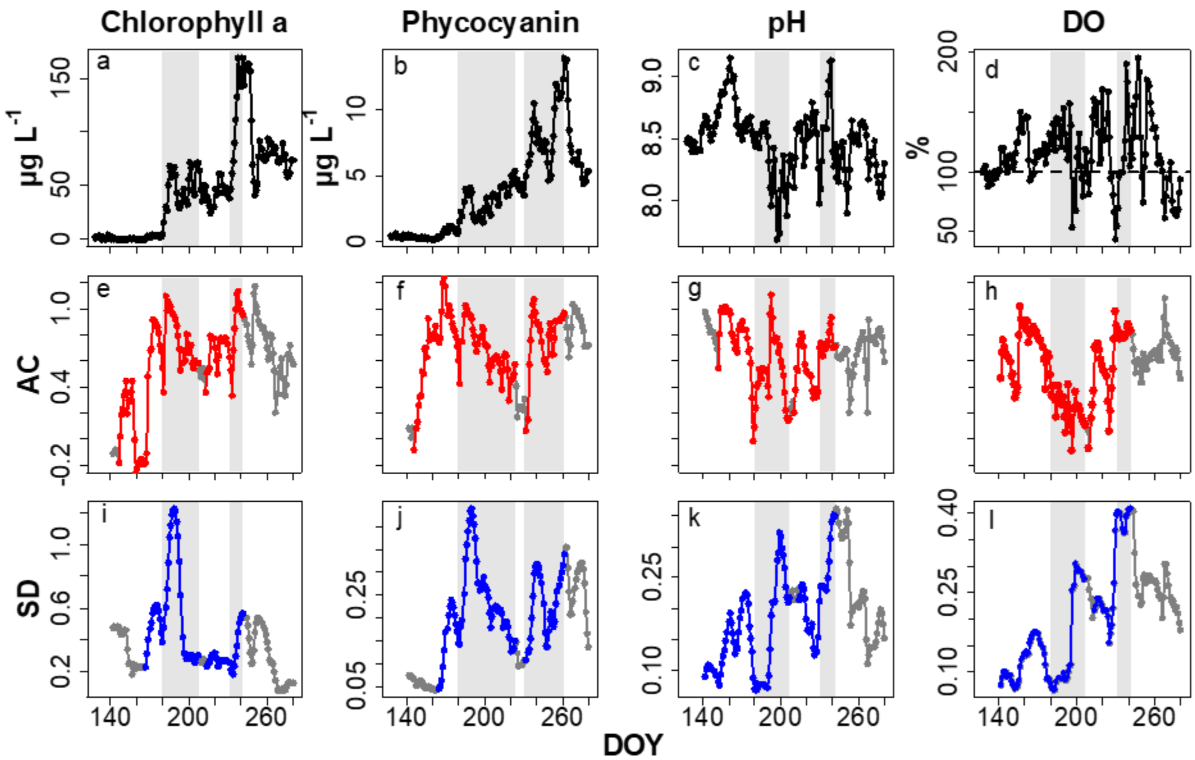

Figure 2.1 Time series of the daily mean of the high frequency data for Blackhawk Lake 2015 for the four state variables (a-d), and the rolling window analysis of autocorrelation (AC) (e-h) and standard deviation (SD) (i-l). The shaded areas extend from the beginning of bloom conditions to the peak biomass of the bloom. Greyed-out lines in the rolling window time series (panels e-i) indicate periods after the bloom when EWIs, by definition, cannot be evaluated. The dashed line in panel d denotes 100% dissolved oxygen saturation.

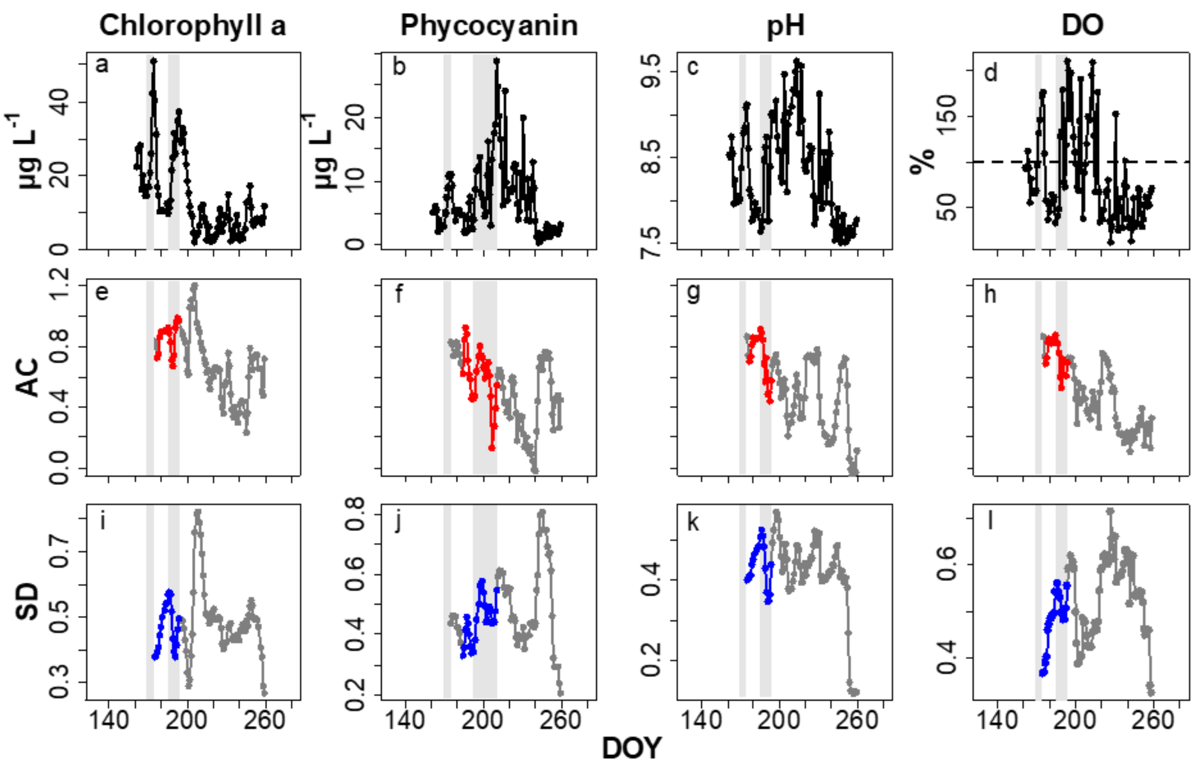

Figure 2.2 Time series of the daily mean of the high frequency data for Green Valley Lake 2014 for the four state variables (a-d), and the rolling window analysis of autocorrelation (AC) (e-h) and standard deviation (SD) (i-l). The shading and line color are the same as Figure 1.1.

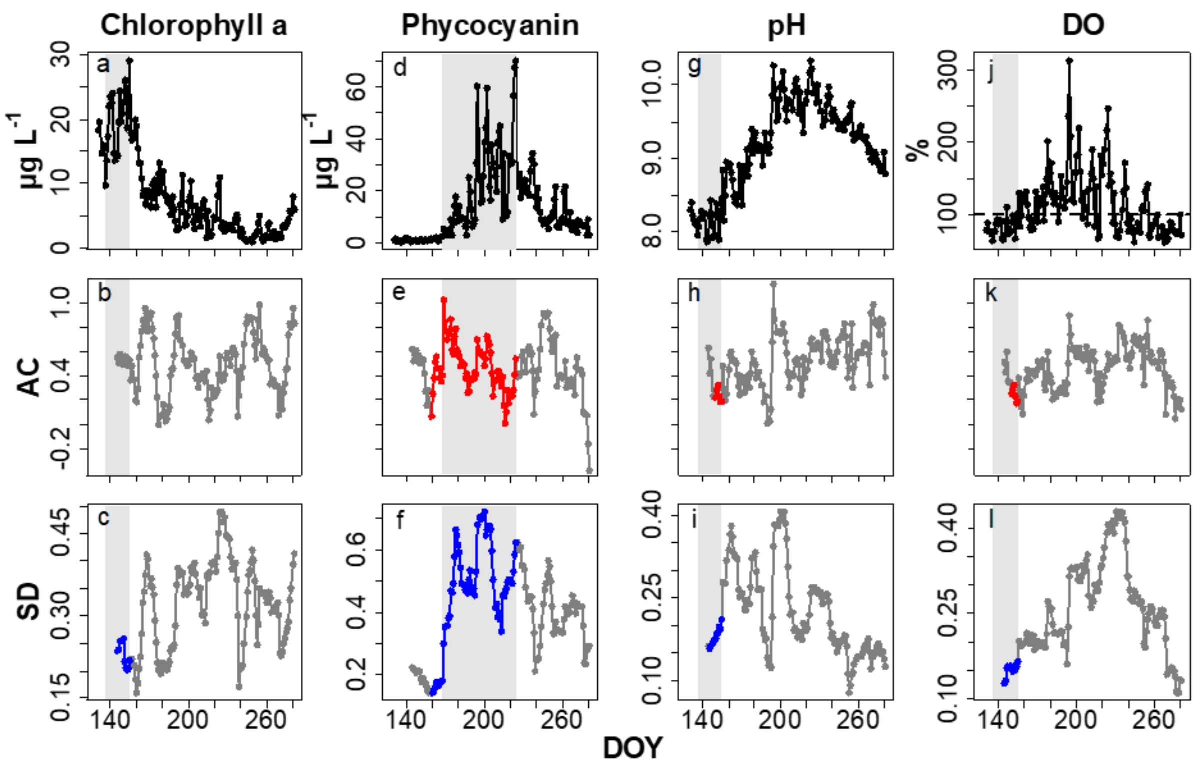

Figure 2.3 Time series of the daily mean of the high frequency data for Green Valley Lake 2015 for the four state variables (a-d), and the rolling window analysis of autocorrelation (AC) (e-h) and standard deviation (SD) (i-l). The shading and line color are the same as Figure 1.1.

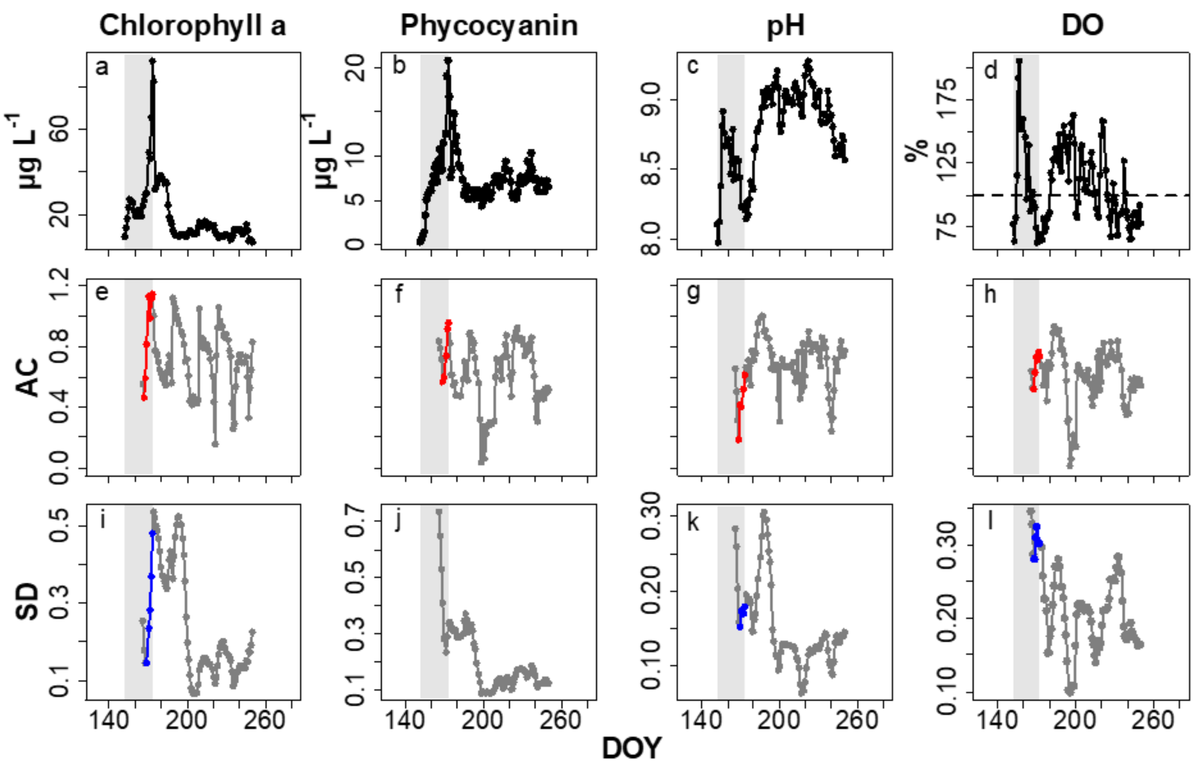

Figure 2.4 Time series of the daily mean of the high frequency data for South Twin Lake 2018 for the four state variables (a-d), and the rolling window analysis of autocorrelation (AC) (e-h) and standard deviation (SD) (i-l). The shading and line color are the same as Figure 1.1.

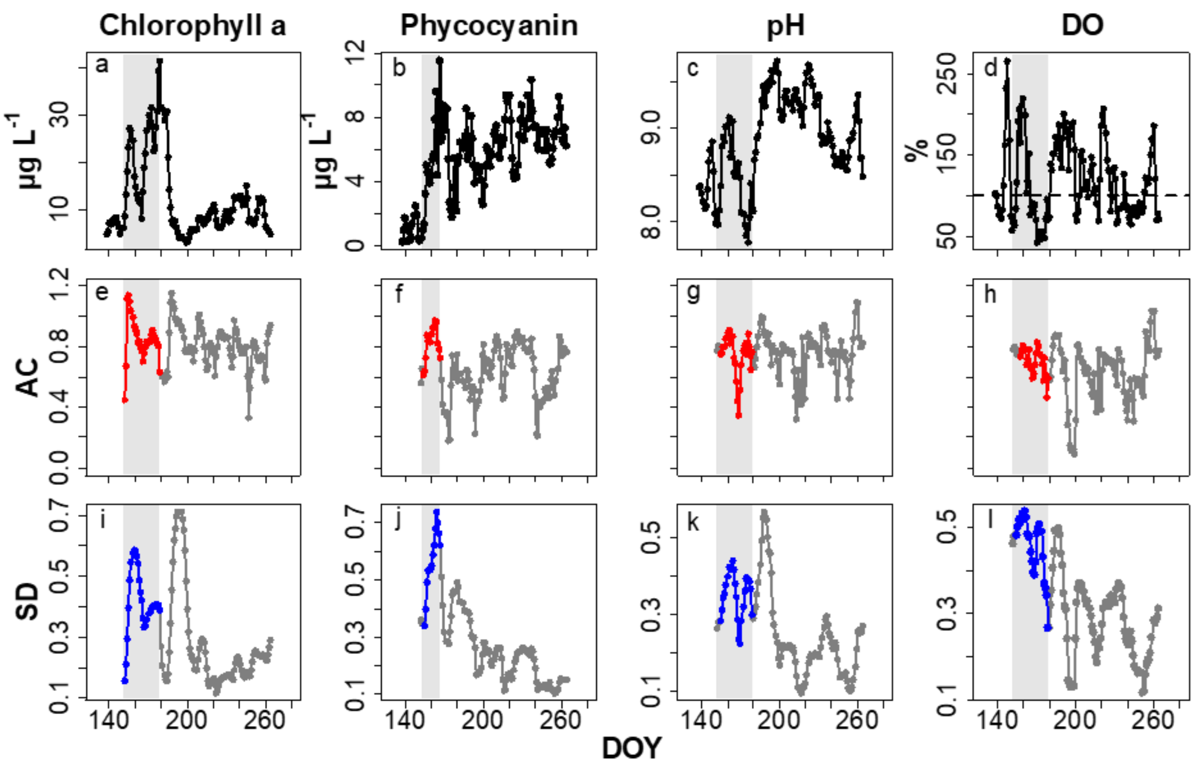

Figure 2.5 Time series of the daily mean of the high frequency data for Swan Lake 2018 for the four state variables (a-d), and the rolling window analysis of autocorrelation (AC) (e-h) and standard deviation (SD) (i-l). The shading and line color are the same as Figure 1.1.

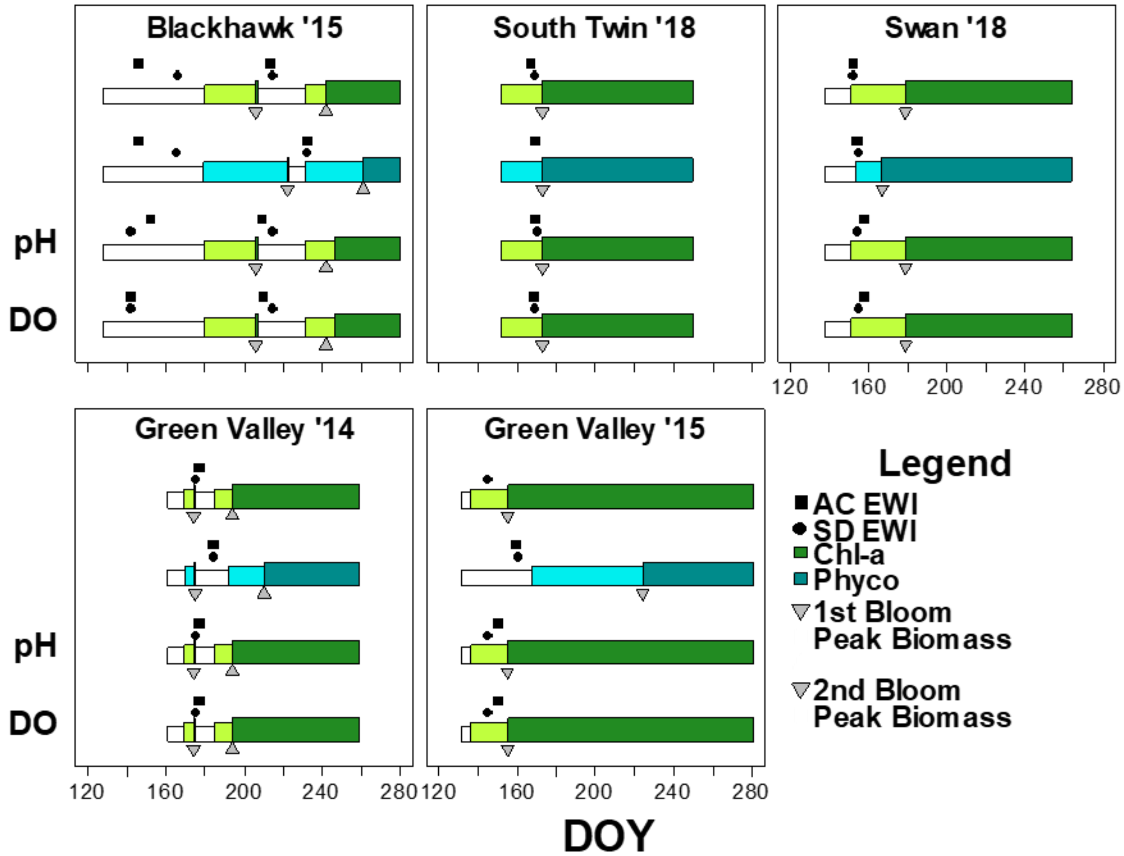

Figure 2.6 The timing of bloom stages (pre-bloom, blooming, peak biomass), and the start of EWIs based on a 15-day rolling window for each state variable in each lake year. The white portion of the timeline and the narrowest bar denotes pre-bloom conditions. The beginning of lighter shades of green or blue in the timeline indicates the start of blooming conditions and ends at peak biomass the 2nd thickest bar, for chlorophyll-a and phycocyanin, respectively. Finally, the darker green or blue portion and thickest bar of the timeline denotes post-bloom conditions after the peak in pigment concentration. The color of the time series indicates if the bloom stages were delineated based on the chlorophyll (green) and phycocyanin (blue) time series. The black rectangles and circles above each timeline indicate the beginning of either the AC EWI or SD EWI, respectively, for that state variable.

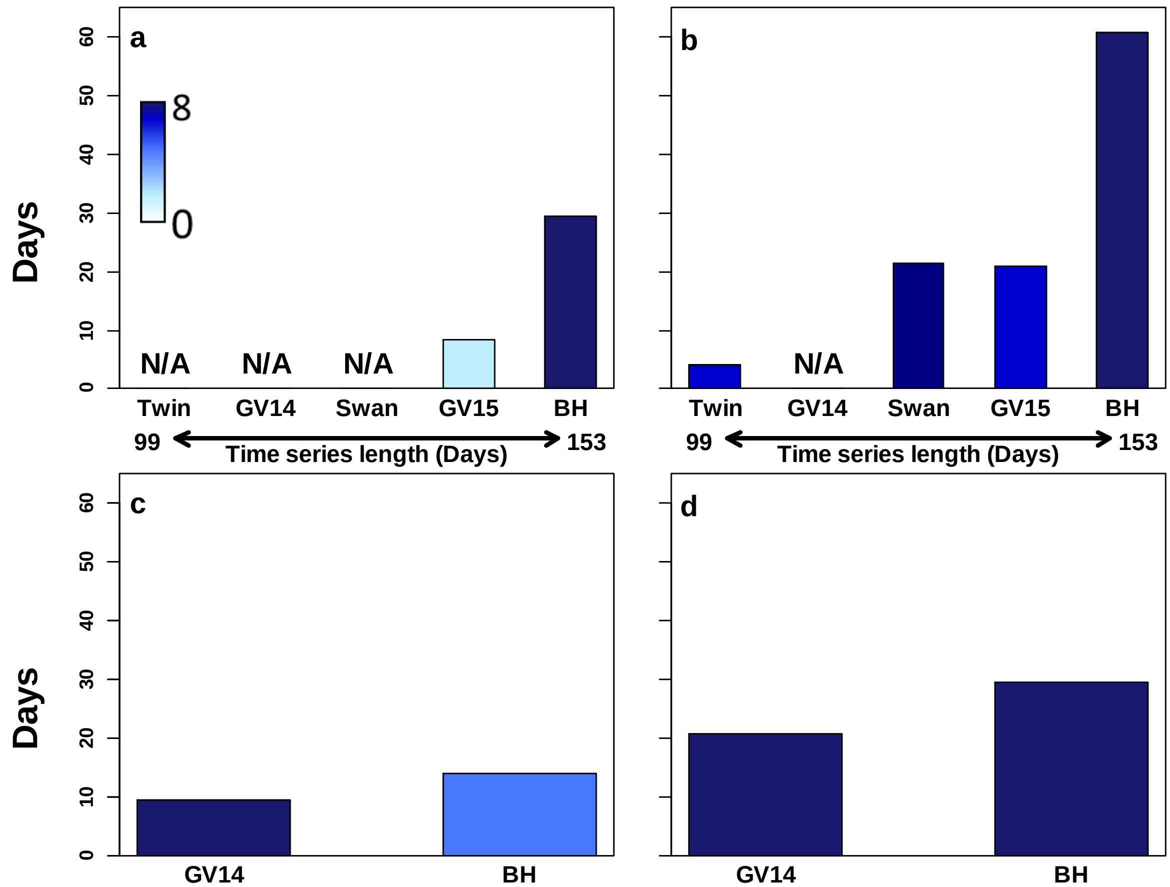

Figure 2.7 Summary of average days EWIs appeared prior to a) bloom conditions and b) before peak biomass for the first bloomSummary of average days prior to c) bloom conditions and d) before peak biomass for second bloom events. The lakes, South Twin (Twin), Green Valley 2014 (GV14), Swan, Green Valley 2015 (GV15), and Blackhawk 2015 (BH), are ordered from smallest time series length to longest, left to right. The color gradient represents the total number of EWIs (out of a possible 8 EWIs) detected before bloom or peak biomass, a darker the bar represents more EWIs detected.

Supplement Figures

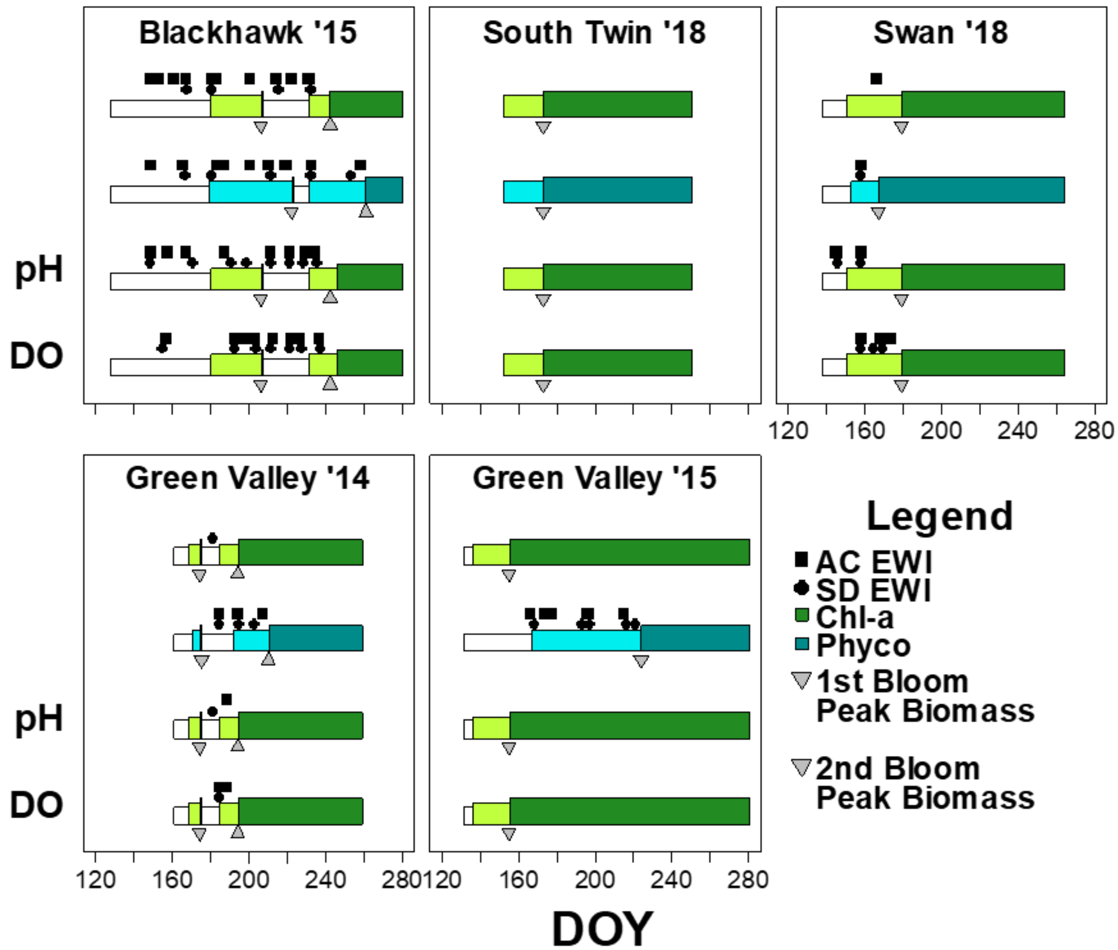

Figure S1.1 The timing of bloom stages (pre-bloom, blooming, peak biomass), and all EWIs based on a 21-day rolling window for each state variable in each lake year. . The white portion of the timeline denotes pre-bloom conditions. The beginning of the light shade of green or blue in the timeline indicates the start of blooming conditions and ends at peak biomass, for chlorophyll-a and phycocyanin, respectively. Finally, the darker green or blue portion of the timeline denotes post-bloom conditions after the peak in pigment concentration. The color of the time series indicates if the bloom stages were delineated based on the chlorophyll (green) or phycocyanin (blue) time series. The black rectangles and circles above each timeline indicate the beginning of either the SD EWI or AC EWI for that state variable.

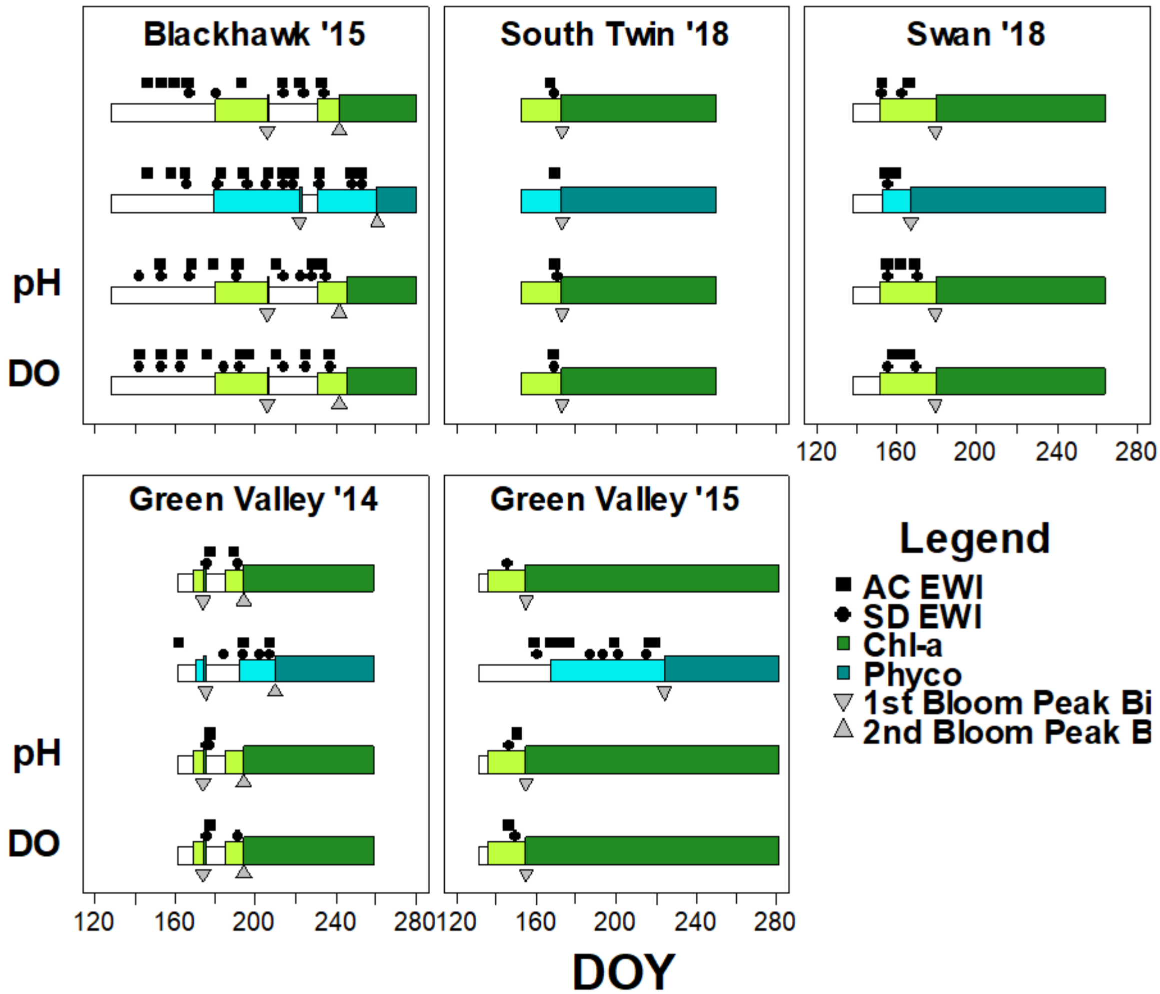

Figure S1.2 The timing of bloom stages (pre-bloom, blooming, peak biomass), and all EWIs based on a 15-day rolling window for each state variable in each lake year. Symbols and coloring are same as S1.

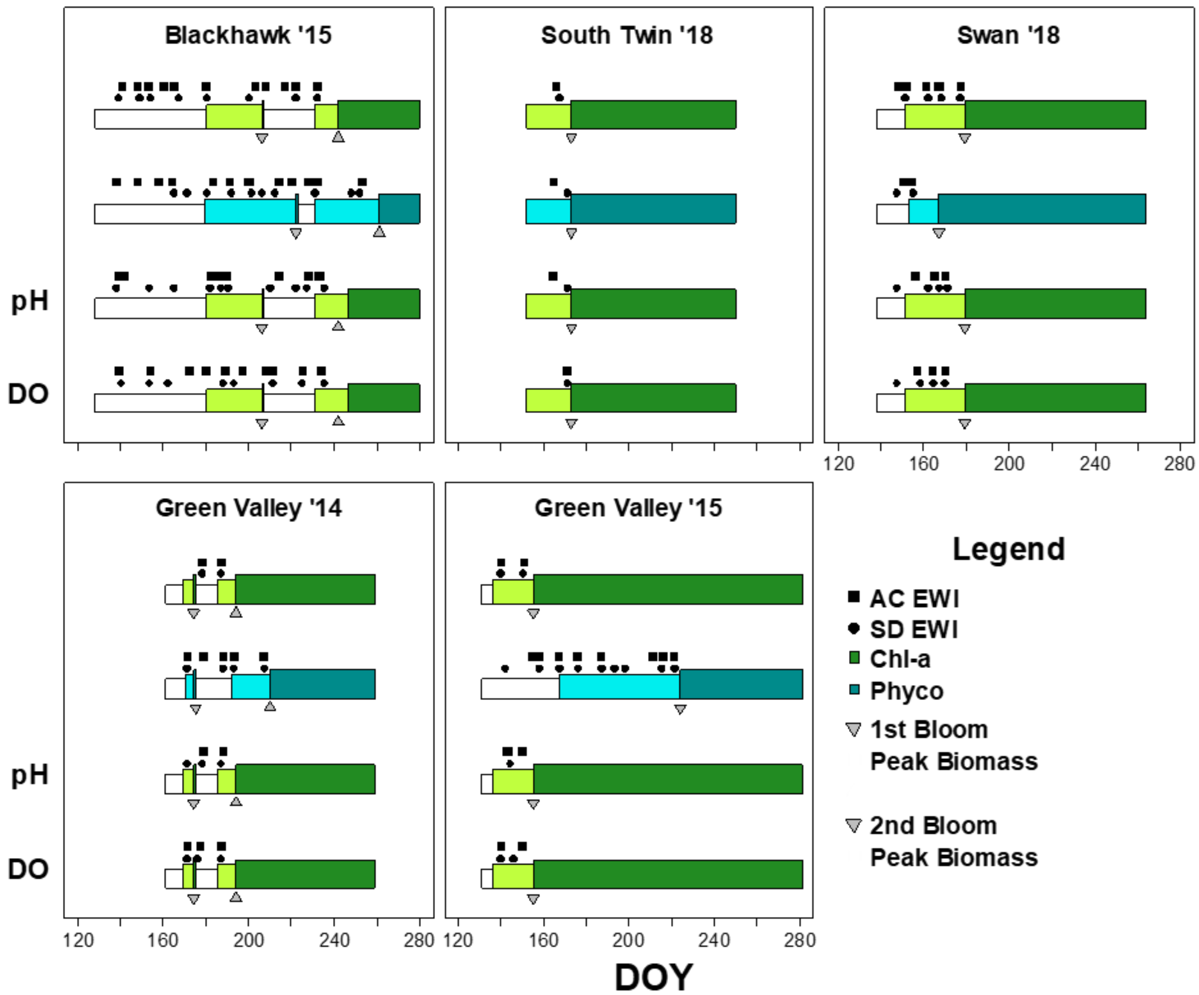

Figure S1.3 The timing of bloom stages (pre-bloom, blooming, peak biomass), and all EWIs based on a 10-day rolling window for each state variable in each lake year. Symbols and coloring are same as S1.

CHAPTER 3. UNDERSTANDING SPATIAL HETEROGENEITY: BEFORE, DURING, AND AFTER AN ALGAL BLOOM

Modified from a manuscript to be submitted to *Ecosphere*
Authors: David Ortiz[1*], Grace Wilkinson[1]
[1]Department of Ecology, Evolution, and Organismal Biology, Iowa State University, Ames, Iowa 50010
*Corresponding Author: daortiz@iastate.edu

Abstract

Monitoring lakes for regime shifts is done using high frequency monitoring at one sample location and interpreted the data to be representative of the entire lake. While single point monitoring has pioneered early warning indicators of oncoming blooms, there are questions regarding spatial heterogeneity of lakes and implications for lake management practices. Detecting evidence of regime shifts in lakes, from clear to algal dominated, spatially has primarily occurred through simulations of ecosystems and only once in lake under experimental conditions. In this study, we empirically tested the use of a weekly spatial sampling scheme in a shallow, spatially complex, and hypereutrophic lake to detect spatial patterns to indicate shifts in regime. Before and during an algal bloom, we saw consistent rise of variance and spatial autocorrelation for chlorophyll-a and phycocyanin. Macrophyte populations are heavily influencing dissolved oxygen and pH making them difficult to interpret as evidence of regime shifts during the second bloom event. Frequent spatial monitoring of an impaired lake produced evidence of a regime shift occurring and occasionally provide an early warning to impending shifts. Moving the early warning indicator field forward from spatial simulations and spatially monitoring experimental lakes to testing the replicability of the phenomenon in non-experimental lakes, as future

implications of spatial monitoring may become a reliable and dynamic tool for lake management.

Introduction

Regime shifts are unexpected transitions between stable states of various ecosystems (Scheffer et al. 2001; Scheffer et al. 2009; Scheffer and Carpenter 2003; Scheffer et al. 2012). Regime shifts are a ubiquitous component of ecosystems, having been detected in food web dynamics (Carpenter et al. 2011; Cline et al. 2014; Gsell et al. 2016; Pace et al. 2013; Seekell et al. 2013), seagrass beds (Ling et al. 2015; van der Heide et al. 2007), forests (Johnstone et al. 2016; Seidl et al. 2016), coral reefs (Hughes et al. 2018; Wernberg et al. 2016), wetlands (Liu et al. 2018), and drylands (D'Odorico et al. 2013; McAllister et al. 2006). Lakes experience regime shifts going from a clear water state to an algal dominated state, also known as harmful algal blooms (HABs) (Carpenter and Brock 2006; Carpenter et al. 2011; Pace et al. 2017; Wilkinson et al. 2018). Ecosystem health is negatively impacted by HABs as they stimulate conditions such as anoxia, light limitation, and possible toxin production (Gilbert 2017; Landsberg 2002). Toxins produced by cyanobacteria during HABs often can rise to dangerous concentrations resulting in nausea, vomiting, and liver damage (Codd et al. 2005; Corbel et al. 2014). What’s more, recreational lake use declines as HABs develop, which in turn can negatively affect local economies (Dodds et al. 2009). As such, a better understanding how and when the HAB regime shift manifests and occurs would allow for more proactive lake management.

Regime shifts can be detected from changes in statistical patterns of state variables over time. For example, a time series of state variables such as algal pigment concentrations collected at one location over time will exhibit a rise in lag-1 autocorrelation (AC) and variance (often measured as standard deviation; SD) prior to the regime shift (Benedetti-

Cecchi et al. 2015; Carpenter and Brock 2006; Pace et al. 2017; Wilkinson et al. 2018). This rise in SD and AC is due to critical slowing down in the system (Scheffer et al. 2009). Similarly, changes in spatial structure as blooms develop (Buelo et al. 2018; Serizawa et al. 2008) produces rises in spatial SD and Moran's I values, which parallels temporal AC, prior to a regime shift (Buelo et al. 2018; Carpenter and Brock 2010; Cline et al. 2014; Dakos et al. 2010; Dakos et al. 2011; Donangelo et al. 2010; Guttal and Jayaprakash 2009). Unlike high frequency (HF) monitoring at one location for extended periods usually at the historical deep point, frequent spatial monitoring in lakes is much less common. More commonly spatial sampling of lakes occurs along transects (Graham et al. 2006; Moreno-Ostos et al. 2009) or is not performed repeatedly to assess changes over time (Sanchis et al. 2002; Wang and Liu 2005; Wu et al. 2010). To our knowledge, the only spatial study of HABs in lakes with adequate spatial coverage and repeated measurements over time occurred under experimental conditions (Butitta et al. 2017).

The single study with evidence of rises in spatial AC and spatial SD prior to a regime shift occurred in a deep, oligotrophic lake that was experimentally eutrophied to induce a cyanobacteria bloom (Butitta et al. 2017). This study served as an initial and important proof-of-concept for spatially detecting rises in spatial AC and SD in a lake; however, the conditions in the experimental lake were not translatable to spatially complex lakes. The experimental ecosystem had naturally low nutrient loading, was bathymetrically simple with a single deep point and strong stratification during the summer, and phytoplankton were the dominant contributors to net ecosystem production dynamics. These characteristics suggests that the lake had high resilience to regime shift causing perturbations, which could be the reason of why detection of rises in spatial AC and SD was possible. Conversely, shallow, hypereutrophic lakes can be spatially complex with large littoral zones dominated by macrophytes, multiple mixing events during the summer, and experience episodic and high nutrient loading (Martin 2003; Pobel et al. 2011; Scheffer and Jeppesen 2007; Scheffer and van Nes 2007). All of these features may interfere with detecting changes in spatial AC and SD prior to a regime shift.

In order to test if regime shifts can be detected spatially in non-experimental lakes we conducted frequent and robust spatial sampling on a shallow, spatially complex, hypereutrophic lake. This lake experienced a large HAB during our sampling which resulted in rises in temporal AC and SD (Ortiz et al. *in prep*). Our sampling scheme included monitoring 98 locations equally spaced out to 65m on a weekly basis, capturing spatial dynamics of our state variables pre, during, and post cyanobacteria blooms. Our goal was to determine if we could detect rises in spatial AC and spatial SD in this spatially complex and impaired ecosystem as evidence of a regime shift.

Methods

Swan Lake (42.0396, -94.8454) has an average depth of 2 m, surface area of 40.5 hectares, watershed of 350 hectares and a shoreline development index value of 1.54. During the ice-free period 2018, Swan Lake had an average total phosphorus concentration of 0.28 mg L^{-1} and a total nitrogen concentration of 2.57 mg L^{-1}, making it hypereutrophic (Clark et al. 2001). Synoptic water quality samples included total nitrogen and phosphorus (Table 1). Total nitrogen was measured as the sum of total Kjeldahl nitrogen (US EPA 1993, method 351.2 v2) and nitrate + nitrite measured using the cadmium reduction method (US EPA 1993, method 4500-NO_3-F). Total phosphorus was measured using the ascorbic acid method (US EPA 1993, method 365.1 v2).

In order to characterize the spatial heterogeneity of state variables before, during, and after a bloom, spatial sampling occurred weekly beginning on day of year (DOY) 135 with the exception of the last two events. The last two sampling periods occurred with two weeks between events, for 17 total spatial sampling events spanning 129 days. To remain consistent with our weekly spatial sampling, measurements were regularly recorded between 9:00 and 14:00, with the first two weeks lasting until 16:00. We used a YSI Pro DSS sonde (Yellow Springs Instrument, Yellow Springs, OH) which was calibrated weekly prior to each sampling event. The sonde was equipped with probes that measured chlorophyll *a*, phycocyanin, dissolved oxygen saturation (DO), pH, and temperature. Measurements were taken at 0.25 m depth at each sampling point. The sampling points on the lake were laid out in a 65x65 meter grid, totaling 98 points (Figure 2.1). We sampled the state variables with the sonde using the same sapling order of points each week from a jon boat. One measurement from weeks 6, 8, 9 and 11 of were removed due to instrument error or possible interference from plant material.

Spatial SD and AC were calculated for each week for each variable to quantify spatial patterns during pre-bloom, bloom, and post-bloom. Spatial AC was calculated as Moran's I, which is a measure of how clustered, dispersed, or random parameter values are across the lake. Specifically, we calculated Moran's I with a queen's distance neighbor list (92 meters) with no weight assumed on neighbors, to not impose any assumptions on any possible spatial patterns of the variables. We limited our analysis to surrounding neighbors because distances beyond this have not shown promising results in experimental conditions (Butitta et al. 2017). Moran's I values near 1.0 reflects high spatial AC within neighbors. Spatial AC values of near 1.0 do not depend on the high or low measured values, just the similarity of a point to its surrounding neighbors. Whereas spatial AC values nearing -1.0 indicate a perfectly dispersed distribution (e.g. checkerboard pattern) of the state variable values. A value of 0.0 indicates a random distribution of the state variable values.

There is not a standard definition for what constitutes an algal bloom. Studies that have provided a definition based it upon a threshold biomass of algae deduced from long-term data with robust observations of the water body in a non-bloom state (Smayda 1997; Wilkinson et al. 2018). Using the changes in algal concentrations over time is an alternative method for defining a blooming period from a HF time series from the historical deep site and supplemented with observations from our spatial sampling. We define a bloom as beginning when pigment concentrations (chlorophyll *a* or phycocyanin) double over the course of five consecutive days or less (Fig. 2.2). We also define the peak of the bloom as the peak concentration of algal biomass based on the peak concentration of pigments. This approach to defining blooms provides definitive pre-bloom, blooming, and bloom periods for ecosystems without historic pigment data. Supplementing our time series bloom definition with the spatial pigment concentrations allows us to become more dynamic and incorporate more information to capture blooms that were failed to be identified with just HF monitoring.

Results

Swan Lake experienced two bloom events in 2018 for both chlorophyll *a* and phycocyanin concentrations. The single-station HF time series captured the first chlorophyll *a* and phycocyanin blooms from DOY 151-179 and DOY 153-167, respectively (Figure 2.2). Similarly, the spatial sampling captured the magnitude of the chlorophyll *a* bloom starting on DOY 156 and extending five days later to DOY 184 (Figure 2.3). Conversely, the spatial phycocyanin measurements had a delayed increase compared to the single-station HF sonde measurements with the bloom beginning on DOY 166; one day before the HF time series indicated the apex of the bloom and extending the bloom duration to DOY 184 (Figure 2.3). While we did not see strong evidence of a second bloom in the single-station HF time series, the spatial sampling suggests that on DOY 236 both pigments were experiencing bloom conditions for a second time in our study period (Figures 2.3 & 2.4).

Spatial Patterns in State Variables

Spatial sampling during the first chlorophyll *a* bloom did not have the expected spatial patterns of rises in spatial AC and SD prior to bloom development. However, as the first chlorophyll *a* bloom ended on DOY 184, there was a gradient of low to high concentrations from west to east and a north to south gradient during the second chlorophyll *a* bloom (Figure 2.3). The highest recorded chlorophyll *a* concentrations were recorded during DOY 184 at 36.6 μg/L at sample site F9 (approximately 250 m from single-station sonde location). The spatial sampling recorded apex values five days prior to the peak concentrations recorded by the HF sonde. Mean chlorophyll *a* concentrations were higher when calculated from the spatial sampling, 9.68 μg L^{-1}, than the single-station HF values for our study period, 5.48 μg L^{-1}.

Spatial phycocyanin concentrations had strong spatial patterns during both bloom periods (Figure 2.4). Phycocyanin concentrations were in a low to high gradient, south to north, throughout most of the sampling period and especially strong during blooms. Northerly sample sites (A1-G4) had higher mean values over the entire summer and during bloom weeks then the southern portion of the lake. The mean phycocyanin concentrations for the duration of the study of the southern portion of the lake was 3.89 μg L^{-1}, while the northern portion was 5.35 μg L^{-1}. During phycocyanin bloom weeks (DOY 166, 170,177,184, and 236) the mean northern concentrations were almost double (7.29 μg L^{-1}) of the southern concentrations (3.76 μg L^{-1}). Phycocyanin concentrations peaked during DOY

184 at 20.5 μg L^{-1} at sampling point B5 (approximately 750 m away from the single-station sonde location), almost doubling the HF data peak concentration of 11.5 μg $L^{-}1$ on DOY 167.

The DO had variable spatial patterns throughout our sampling period, shifting general spatial gradients over time and had consistently low and high saturation locations (Figure 2.5). During the first chlorophyll *a* – based bloom apex, there was a gradient of low to high DO saturations from south to north on DOY 184. There were consistently low DO values recorded surrounding sample point D6, noticeably from DOY 198 – 226. There was a large range of DO values, with the highest recorded value at 352 % on DOY 184 at point C5 and the lowest at 30.5% on DOY 236 at A1 (Figure 2.5). After the first bloom subsided DO values persisted at high saturations (approximately 150%) until the last sampling event on DOY 264. Conversely, the maximum value recorded by the single-station HF time series was 266% on DOY 145, illustrating the lake wide heterogeneity in DO saturation in both space and time.

Spatial pH values also had strong low to high gradients along a south to north pattern, especially during both chlorophyll *a* – based blooms and following the second bloom event (Figure 2.6). The strongest south to north gradient in pH was recorded on DOY 166 with a mean pH of 9.12 in the northern portion of the lake and mean pH of 8.55 in the southern portion. The highest recorded value of pH was 9.93 on DOY 191 at both C11 and E4, while the largest pH value in the single-station HF time series was recorded seven days later at 9.73. After DOY 191, Swan Lake maintained high pH values across the entire lake through DOY 226.

Evidence of Regime Shifts in Spatial Data

Spatial AC values ranged from 0.0 (perfect randomness) to 0.8 (near-perfect correlation) amongst all of the state variables, indicating that there were no instances of high dispersion (Figures 2.7a, c, e, g). There were differences in the time series of spatial AC amongst chlorophyll *a* and phycocyanin before the first bloom event. There was a rise in spatial AC of chlorophyll *a* during the first two weeks of sampling prior to the first bloom, with the highest values of AC shortly after the bloom began on DOY 166 (Figure 2.7a). Conversely, phycocyanin spatial AC began to rise two sampling events prior to the bloom and peaked during the end of the bloom on DOY184. Chlorophyll *a* spatial AC had a dampened response to the second bloom event, starting to rise in the middle of the bloom and peaking after it ended on DOY 250. However, phycocyanin spatial AC responded to the second bloom by rising during the one spatial sampling event that captured the height of the bloom (Figure 2.7c).

The trends in spatial AC of DO and pH were similar during the course of the summer (Figures 2.7 e & g). For the first bloom event both DO and pH spatial AC dropped at the beginning of the bloom, and peaked in the second spatial sampling event after the bloom had begun, DOY 166, as did the chlorophyll *a*. During the single spatial sampling event that captured the second bloom, both DO and pH spatial AC rose similarly to that of that phycocyanin spatial AC.

Chlorophyll *a* and phycocyanin SD began to rise one week into their respective bloom events with both peaking during the last spatial sampling event within the bloom on DOY 156 and 166 (Figures 2.7b & d). Similarly, the DO- and pH-based SD began to rise one week prior to the first chlorophyll *a* bloom and peaked during the last spatial sampling event within the bloom on DOY 184 (Figures 2.7f & h). The values of chlorophyll *a* SD began to rise four weeks prior the second bloom event and peaked during the one spatial sampling event that occurred during the second bloom (Figure 2.7b). Phycocyanin SD only rose during the sampling event that occurred during the second bloom (Figure 2.7b), while DO and pH did not express rises in SD for the second chlorophyll *a* bloom event. There was a decline in DO-based SD from DOY 212, through the second bloom, and to the end of study period (Figure 2.7f). During first bloom pH-based SD rose and then remained constant though the second bloom and through the end of the study period (Figure 2.7h).

Overall, spatial AC had delayed rises at the beginning of each bloom for each state variable, with the exception of phycocyanin during the first bloom event (Figures 2.7a,c,e,g). Delayed spatial AC for chlorophyll *a*, DO and pH rose during the second spatial sampling week into the first bloom event, while phycocyanin stared to rise the week before the first bloom occurred. All state variables rose in spatial AC for the second bloom event, indicating the distribution of the state variables went from an almost perfectly random distribution to higher spatial correlation, with the exception of chlorophyll *a*. All state variables rose in SD at least one spatial sampling event before the first bloom event, with the exception of chlorophyll *a* that rose during the first spatial sampling at the beginning of the bloom (Figures 2.7b, d, f, h). We anticipated rises in SD prior to the second bloom event as well, chlorophyll *a* and phycocyanin both responded as we expected. Chlorophyll *a* began to rise in SD four sampling events prior to the second bloom and phycocyanin SD rose during the sampling event during the second bloom. On the other hand, DO-based SD dropped beginning three sampling events (DOY 212) prior to the second chlorophyll *a* bloom through the end of the study period and pH-based SD remained stagnant from DOY 205 onward.

Discussion

This study demonstrates the possibility of detecting rises in spatial AC and SD of state variables prior to a regime shift in a shallow hypereutrophic lake. There were two bloom events during the summer of 2018 in Swan Lake providing us ample opportunities to test the hypothesis that spatial SD and AC rises can be detected as evidence of regime shift (Buelo et al. 2018; Butitta et al. 2017; Dakos et al. 2010). All four state variables we monitored chlorophyll *a*, phycocyanin, DO, and pH expressed rises in spatial AC as blooms were occurring, with the exception of phycocyanin, which began to rise even earlier (ten days) prior to the first bloom event. The phycocyanin-based spatial AC surpassed our expectations and could be interpreted as an early warning indicator to the oncoming bloom. All variables responded similarly for the second bloom for spatial AC, rising as the bloom occurred. Phycocyanin, DO, and pH-based spatial SD rose prior to the first bloom also serving as early warnings to the first bloom. On the other hand, chlorophyll *a*-based spatial SD also rose during spatial sampling events that occurred during the bloom. For the second bloom, the pigments responded strongly with rises in spatial SD, but DO and pH did not rise as we anticipated. Chlorophyll *a* – based spatial SD began to rise 31 days prior to the start of the second bloom, providing use with the most timely interpretable early warning. These rises in spatial AC and SD are may not be consistent enough to serve as reliable early warning indicators to an oncoming regime shift (Buttita et al. 2017; Dakos et al. 2010), but the results from this study are insightful for understanding spatial patterns of bloom in spatially complex lakes and provide evidence of detecting regime shifts spatially.

Unlike recent spatial regime shift research in lakes (Buttita et al. 2017; Cline et al. 2014), our study lake was shallow, hypereutrophic, spatially complex, and experienced ambient, heterogeneous nutrient loading dynamics. In particular, our study lake had embayments, a large littoral zone, and surface inlets and an outlet which contributed to the spatial complexity and likely influence the patterns of spatial heterogeneity in the state variables. The spatial structure of our study lake is in sharp contrast to the lake in which the proof-of-concept study that provided evidence of detecting rises in spatial AC and SD under experimental nutrient enrichment (Butitta et al. 2017). That ecosystem, Peter Lake, has a simple bathymetry with a relatively small littoral zone, no surface inlets, limited macrophyte populations (Carpenter and Kitchell 1995), and monitored at an amazingly fine scale (Butitta et al. 2017). As such, it is possible that the lack of spatial complexity compared to Swan Lake will have made the spatial SD and AC dynamics easier to detect prior to a bloom. However, this study demonstrated that these signals are detectable in more spatially complex lakes on a 65m sampling grid.

A major confounding factor to detecting rises in spatial AC and SD for DO and pH was the presence of macrophytes beds in Swan Lake (Carpenter and Lodge 1986; Carter et al. 1991; Frieder et al. 2012). Submerged macrophytes photosynthesize which produces and releases dissolved oxygen into water column. Much of the northern portion (sites A1-G9) of Swan Lake was covered in macrophyte beds of sago pondweed (*Stuckenia pectinate*) spanning an estimated area of 32 hectares and an American lotus (*Nelumbo lutea*) patch about one hectare from DOY 177 through the end of the sampling period. For Swan Lake, it was necessary to compliment the spatial and temporal data with robust macrophyte surveys in order to interpret the spatial patterns, but also the rises in spatial AC and SD. Future spatial regime shift research needs to be paired with detailed habitat sampling to interpret the spatial dynamics of the state variables. The presence of macrophytes also has an impact on pH values. As dissolved carbon dioxide is removed from the water column by photosynthesis, this decreases the amount of carbonic acid thereby causing pH to increase. The primary productivity of macrophytes can also explain the spatial pattern of DO and pH and the dynamics of the spatial statistics. On the other hand, the decomposition of algal and macrophyte biomass could have contributed to the declines in DO and pH values from DOY 198 through the end of the sampling period. This calls into question the assurance of what and how DO and pH-based rises in spatial SD and AC are truly conveying regarding evidence of an algae-based regime shift.

Some the characteristics of cyanobacteria, such as surface scums and manipulating of their buoyancy (Cui et al. 2016; Klemer et al. 1996) could lead to over and under estimation of biomass. The sonde used for spatial sampling was positioned ~0.25 m in the water column. The dense populations of macrophytes may have also had impacts on where higher concentrations of chlorophyll *a* and phycocyanin were recorded. The dense macrophyte beds seemed to dramatically reduce the movement of water and possibly created stagnate areas of water. These areas of stagnation may have been more favorable to cyanobacteria growth. In addition to creating stagnant pockets of water, macrophytes may have served as surfaces for algae to cling on to and grow. The stationary HF sonde is insightful for several monitoring purposes but becomes an inadequate representation of conditions in large, complex ecosystems. However, spatial monitoring of water quality parameters has the opportunity to capture the heterogeneity of conditions and possibly reveal patterns and drivers of dynamics across the lake.

The potential knowledge gained from spatial monitoring is not limited to detecting rises in spatial AC and SD but also to better understand how state variables behave across the entire lake. Our study identified two bloom periods in our dataset, the first bloom for both chlorophyll *a* and phycocyanin were identified by the high frequency times series deployed at site H2 (Figure 2.2). The first bloom period agreed with the spatial data, showing increases in state variables, while the second bloom did not appear particularly strong in the single-station HF time series but did appear in our spatial data (Figures 2.3 & 2.4). The supplementation of spatial information to the time series data yielded a more robust contextualization of a bloom across the entire lake. Another example, more applicable to lake management, is a spatial understanding of a lake allows for the identification of hot spots that may need more management attention in the lake and areas that are less of a biological concern. For example, the strong gradients in the algal pigments from north to south could be used to design where toxin monitoring should occur to capture the true exposure threat while minimizing costs. Identifying areas with high pH could also signal areas to monitor for additional issues such as reduced fish reproduction (Alavi and Cosson 2006), deadly concentrations of unionized ammonia concentrations which may harm fish (Mooney et al. 2019), and perception of carbonate (Dupraz et al. 2009). Areas identified to have consistently low DO could also be candidates for special management treatment (e.g. aeration) to avoid fish kills.

Spatial sampling was able to detect distinct rises in both spatial AC and SD in pigment concentrations before and during regime shifts with a weekly sampling scheme on a coarse sampling grid of 65 meters. Providing supporting evidence to both theorized and experimental lake studies that have detected regime shifts spatially and evidence of predictive power in some of our state variables in a non-experimental lake. However, spatial patterns from pH and DO did not exhibit the expected patterns suggesting a regime shift due to the presence of macrophytes during the second half of the sampling period. This study although insightful for the implication of spatial sampling as an additional tool to detect regime shifts brings to light several new knowledge gaps. Can the number of sample locations and variables monitored be reduced and still detect informative rises in spatial AC and SD? Is there a scalable relationship between the number of sample locations and lake size? What does the spatial resolution need to be for assessing other sources of net ecosystem production and how often does the assessment need to occur? May the identification of these new knowledge gaps and the success of detecting regime shifts in this study be a call to action for the implication and exploration of spatial monitoring in novel ecosystems. Providing empirical evidence that the detection of regime shifts spatially is possible in a heavily impaired waterbody, we move forward the field of simulations and experimental lake monitoring to testing the replicability of the phenomenon.

Acknowledgments

We would like to thank Ryan Wagner, Ellen Albright, and Tyler Butts for assistance with data collection for instrument deployment and collection. We would also like to thank Rachel Fleck for water sample processing guidance. Funding provided by the Center for Global and Regional Environmental Research, the Iowa State University Graduate Minority Assistantship Program, and the Iowa State University Graduate Research Assistantship Match Program.

References

Alavi, S. M. H., and J. Cosson. 2006. Sperm motility in fishes. (II) Effects of ions and osmolality: A review. Cell Biology International **30:** 1-14.

Benedetti-Cecchi, L., L. Tamburello, E. Maggi, and F. Bulleri. 2015. Experimental Perturbations Modify the Performance of Early Warning Indicators of Regime Shift. Current Biology **25:** 1867-1872.

Buelo, C. D., S. R. Carpenter, and M. L. Pace. 2018. A modeling analysis of spatial statistical indicators of thresholds for algal blooms. Limnology and Oceanography Letters **3:** 384-392.

Butitta, V. L., S. R. Carpenter, L. C. Loken, M. L. Pace, and E. H. Stanley. 2017. Spatial early warning signals in a lake manipulation. Ecosphere **8**. DOI: 10.1002/ecs2.1941

Carpenter, S. R., and W. A. Brock. 2006. Rising variance: a leading indicator of ecological transition. Ecology Letters **9:** 308-315.

---. 2010. Early warnings of regime shifts in spatial dynamics using the discrete Fourier transform. Ecosphere **1**. DOI: 10.1890/ES10-00016.1

Carpenter, S. R. and others 2011. Early Warnings of Regime Shifts: A Whole-Ecosystem Experiment. Science **332:** 1079-1082.

Carpenter, S. R., and D. M. Lodge. 1986. Effects Of Submersed Macrophytes On Ecosystem Processes. Aquatic Botany **26:** 341-370.

Carpenter, S. R. and J. F. Kitchell. 1995. *The trophic cascade in lakes.* USA: Cambridge University Press.

Carter, V., N. B. Rybicki, and R. Hammerschlag. 1991. Effects Of Submersed Macrophytes On Dissolved-Oxygen, Ph, And Temperature Under Different Conditions Of Wind, Tide, And Bed Structure. Journal of Freshwater Ecology **6:** 121-133.

Clark, J. S. and others 2001. Ecological forecasts: An emerging imperative. Science **293:** 657-660.

Cline, T. J. and others 2014. Early warnings of regime shifts: evaluation of spatial indicators from a whole-ecosystem experiment. Ecosphere **5**. DOI: 10.1890/es13-00398.1.

Codd, G. A., L. F. Morrison, and J. S. Metcalf. 2005. Cyanobacterial toxins: risk management for health protection. Toxicology and Applied Pharmacology **203:** 264-272.

Corbel, S., C. Mougin, and N. Bouaicha. 2014. Cyanobacterial toxins: Modes of actions, fate in aquatic and soil ecosystems, phytotoxicity and bioaccumulation in agricultural crops. Chemosphere **96:** 1-15.

Cui, Y. J. and others 2016. Diel migration of Microcystis during an algal bloom event in the Three Gorges Reservoir, China. Environmental Earth Sciences **75**. DOI: 10.1007/s12665-015-5124-x

D'Odorico, P., A. Bhattachan, K. F. Davis, S. Ravi, and C. W. Runyan. 2013. Global desertification: Drivers and feedbacks. Advances in Water Resources **51:** 326-344.

Dakos, V., S. Kefi, M. Rietkerk, E. H. van Nes, and M. Scheffer. 2011. Slowing Down in Spatially Patterned Ecosystems at the Brink of Collapse. American Naturalist **177:** E153-E166.

Dakos, V., E. H. van Nes, R. Donangelo, H. Fort, and M. Scheffer. 2010. Spatial correlation as leading indicator of catastrophic shifts. Theoretical Ecology **3:** 163-174.

Dodds, W. K. and others 2009. Eutrophication of US Freshwaters: Analysis of Potential Economic Damages. Environmental Science & Technology **43:** 12-19.

Donangelo, R., H. Fort, V. Dakos, M. Scheffer, and E. H. Van Nes. 2010. Early Warnings For Catastrophic Shifts In Ecosystems: Comparison Between Spatial And Temporal Indicators. International Journal of Bifurcation and Chaos **20:** 315-321.

Dupraz, C., R. P. Reid, O. Braissant, A. W. Decho, R. S. Norman, and P. T. Visscher. 2009. Processes of carbonate precipitation in modern microbial mats. Earth-Science Reviews **96:** 141-162.

Frieder, C. A., S. H. Nam, T. R. Martz, and L. A. Levin. 2012. High temporal and spatial variability of dissolved oxygen and pH in a nearshore California kelp forest. Biogeosciences **9:** 3917-3930.

Gilbert, P. M. 2017. Eutrophication, harmful algae and biodiversity - Challenging paradigms in a world of complex nutrient changes. Marine Pollution Bulletin **124:** 591-606.

Graham, J. L., J. R. Jones, S. B. Jones, and T. E. Clevenger. 2006. Spatial and temporal dynamics of microcystin in a Missouri reservoir. Lake and Reservoir Management **22:** 59-68.

Gsell, A. S. and others 2016. Evaluating early-warning indicators of critical transitions in natural aquatic ecosystems. Proceedings of the National Academy of Sciences of the United States of America **113:** E8089-E8095.

Guttal, V., and C. Jayaprakash. 2009. Spatial variance and spatial skewness: leading indicators of regime shifts in spatial ecological systems. Theoretical Ecology **2:** 3-12.

Hughes, T. P. and others 2018. Spatial and temporal patterns of mass bleaching of corals in the Anthropocene. Science **359:** 80-83.

Johnstone, J. F. and others 2016. Changing disturbance regimes, ecological memory, and forest resilience. Frontiers in Ecology and the Environment **14:** 369-378.

Klemer, A. R., J. J. Cullen, M. T. Mageau, K. M. Hanson, and R. A. Sundell. 1996. Cyanobacterial buoyancy regulation: The paradoxical roles of carbon. Journal of Phycology **32:** 47-53.

Landsberg, J. H. 2002. The effects of harmful algal blooms on aquatic organisms. Reviews in Fisheries Science **10:** 113-390.

Ling, S. D. and others 2015. Global regime shift dynamics of catastrophic sea urchin overgrazing. Philosophical Transactions of the Royal Society B-Biological Sciences **370**. DOI: 10.1098/rstb.2013.0269

Liu, H. X., C. Y. Gao, and G. P. Wang. 2018. Understand the resilience and regime shift of the wetland ecosystem after human disturbances. Science of the Total Environment **643:** 1031-1040.

Martin, A. P. 2003. Phytoplankton patchiness: the role of lateral stirring and mixing. Progress in Oceanography **57:** 125-174.

McAllister, R. R. J., I. J. Gordon, M. A. Janssen, and N. Abel. 2006. Pastoralists' responses to variation of rangeland resources in time and space. Ecological Applications **16:** 572-583.

Mooney, T. J. and others 2019. Freshwater chronic ammonia toxicity: A tropical-to-temperate comparison. Environmental Toxicology and Chemistry **38:** 177-189.

Moreno-Ostos, E., L. Cruz-Pizarro, A. Basanta, and D. G. George. 2009. Spatial Heterogeneity of Cyanobacteria and Diatoms in a Thermally Stratified Canyon-Shaped Reservoir. International Review of Hydrobiology **94:** 245-257.

Pace, M. L. and others 2017. Reversal of a cyanobacterial bloom in response to early warnings. Proceedings of the National Academy of Sciences of the United States of America **114:** 352-357.

Pace, M. L., S. R. Carpenter, R. A. Johnson, and J. T. Kurtzweil. 2013. Zooplankton provide early warnings of a regime shift in a whole lake manipulation. Limnology and Oceanography **58:** 525-532.

Pobel, D., J. Robin, and J. F. Humbert. 2011. Influence of sampling strategies on the monitoring of cyanobacteria in shallow lakes: Lessons from a case study in France. Water Research **45:** 1005-1014.

Sanchis, D. and others 2002. Spatial and temporal heterogeneity in succession of cyanobacterial blooms in a Spanish reservoir. Annales De Limnologie-International Journal of Limnology **38:** 173-183.

Scheffer, M. and others 2009. Early-warning signals for critical transitions. Nature **461:** 53-59.

Scheffer, M., S. Carpenter, J. A. Foley, C. Folke, and B. Walker. 2001. Catastrophic shifts in ecosystems. Nature **413:** 591-596.

Scheffer, M., and S. R. Carpenter. 2003. Catastrophic regime shifts in ecosystems: linking theory to observation. Trends in Ecology & Evolution **18:** 648-656.

Scheffer, M. and others 2012. Anticipating Critical Transitions. Science **338:** 344-348.

Scheffer, M., and E. Jeppesen. 2007. Regime shifts in shallow lakes. Ecosystems **10:** 1-3.

Scheffer, M., and E. H. van Nes. 2007. Shallow lakes theory revisited: various alternative regimes driven by climate, nutrients, depth and lake size. Hydrobiologia **584:** 455-466.

Seekell, D. A., T. J. Cline, S. R. Carpenter, and M. L. Pace. 2013. Evidence of alternate attractors from a whole-ecosystem regime shift experiment. Theoretical Ecology **6:** 385-394.

Seidl, R., T. A. Spies, D. L. Peterson, S. L. Stephens, and J. A. Hicke. 2016. Searching for resilience: addressing the impacts of changing disturbance regimes on forest ecosystem services. Journal of Applied Ecology **53:** 120-129.

Serizawa, H., T. Amemiya, and K. Itoh. 2008. Patchiness in a minimal nutrient - phytoplankton model. Journal of Biosciences **33:** 391-403.

Smayda, T. J. 1997. What is a bloom? A commentary. Limnology and Oceanography **42:** 1132-1136.

United States Environmental Protection Agency. 1993. Determination of Nitrate-Nitrite by Automated Colorimetry. Method 353.2 Revision 2.0.

United States Environmental Protection Agency. 1993. Determination of Phosphorus by Semi-Automated Colorimetry. Method 365.1 Revision 2.0.

United States Environmental Protection Agency. 1993. Determination of Total Kjeldahl Nitrogen by Semi-Automated Colorimetry. Method 351.2 Revision 2.0.

van der Heide, T., E. H. van Nes, G. W. Geerling, A. J. P. Smolders, T. J. Bouma, and M. M. van Katwijk. 2007. Positive feedbacks in seagrass ecosystems: Implications for success in conservation and restoration. Ecosystems **10:** 1311-1322.

Wang, X. J., and R. M. Liu. 2005. Spatial analysis and eutrophication assessment for chlorophyll a in Taihu Lake. Environmental Monitoring and Assessment **101:** 167-174.

Wernberg, T. and others 2016. Climate-driven regime shift of a temperate marine ecosystem. Science **353:** 169-172.

Wilkinson, G. M. and others 2018. Early warning signals precede cyanobacterial blooms in multiple whole-lake experiments. Ecological Monographs **88:** 188-203.

Wu, X. D. and others 2010. Horizontal distribution and transport processes of bloom-forming Microcystis in a large shallow lake (Taihu, China). Limnologica **40:** 8-15.

Figures

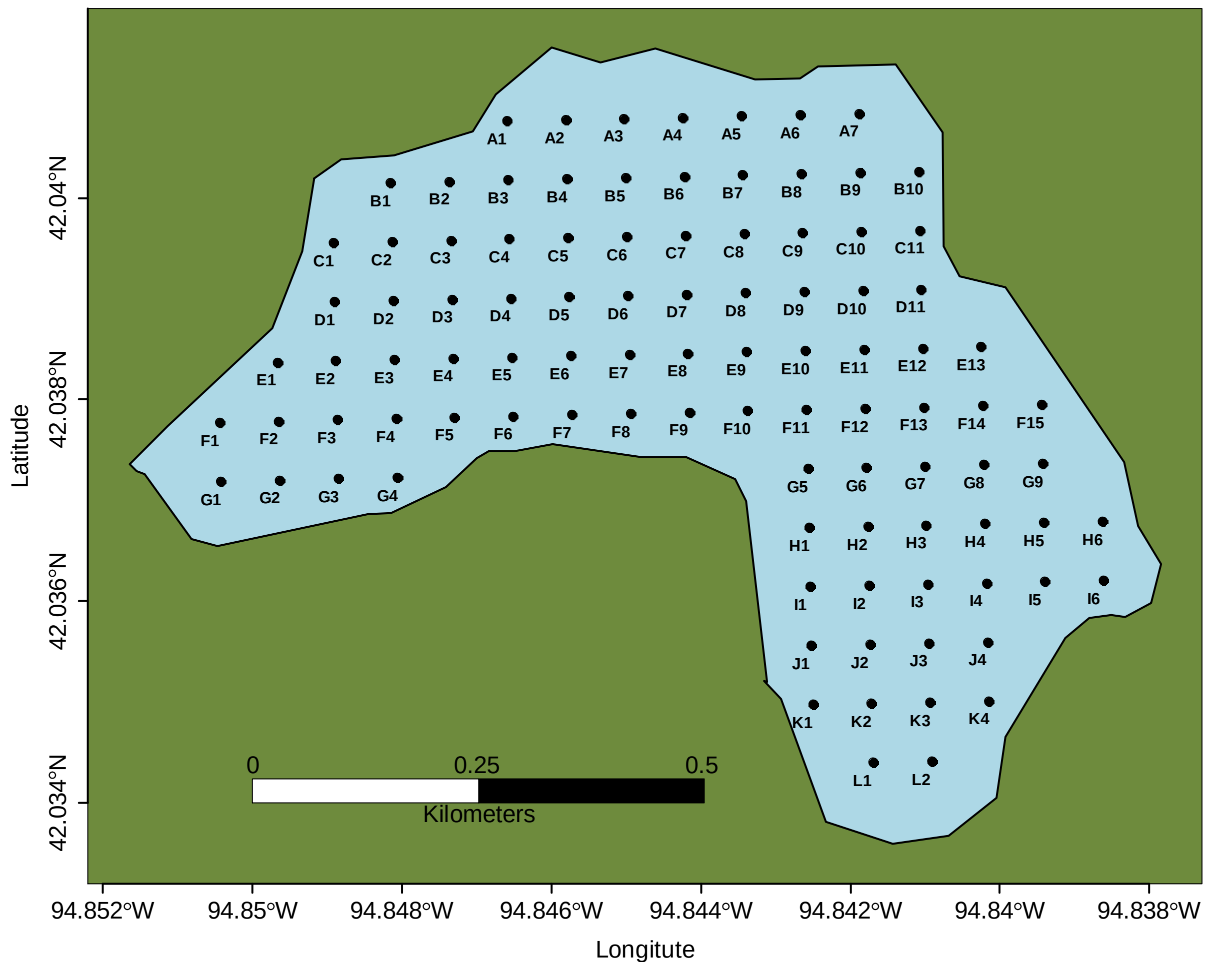

Figure 3.1 The spatial sampling locations on Swan Lake and the alphanumeric labeling scheme. The main inlet is located the on the most western point of the lake, and the outlet is located at the most southern point of the lake. Sampling location H2 is the historical deep point.

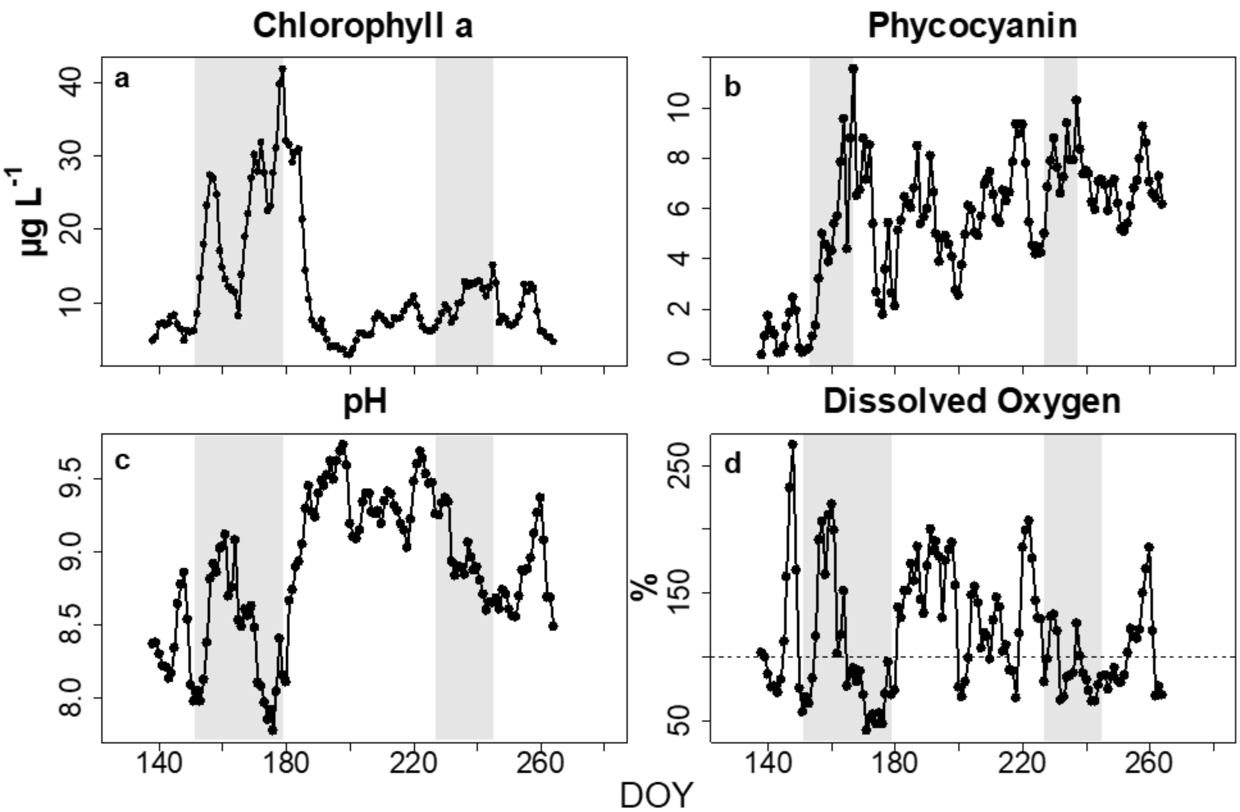

Figure 3.2 Time series from high frequency sonde to indicate pre, bloom, and post bloom conditions for a) chlorophyll *a*, b) phycocyanin, c) pH, and d) percent saturation dissolved oxygen. Bloom periods are indicated with grey shading, ph and dissovled oxygen shaded areas are in reference to chlorophyll *a* bloom periods. Horizontial dashed line in panel d is representative of 100% dissolved oxygen saturation.

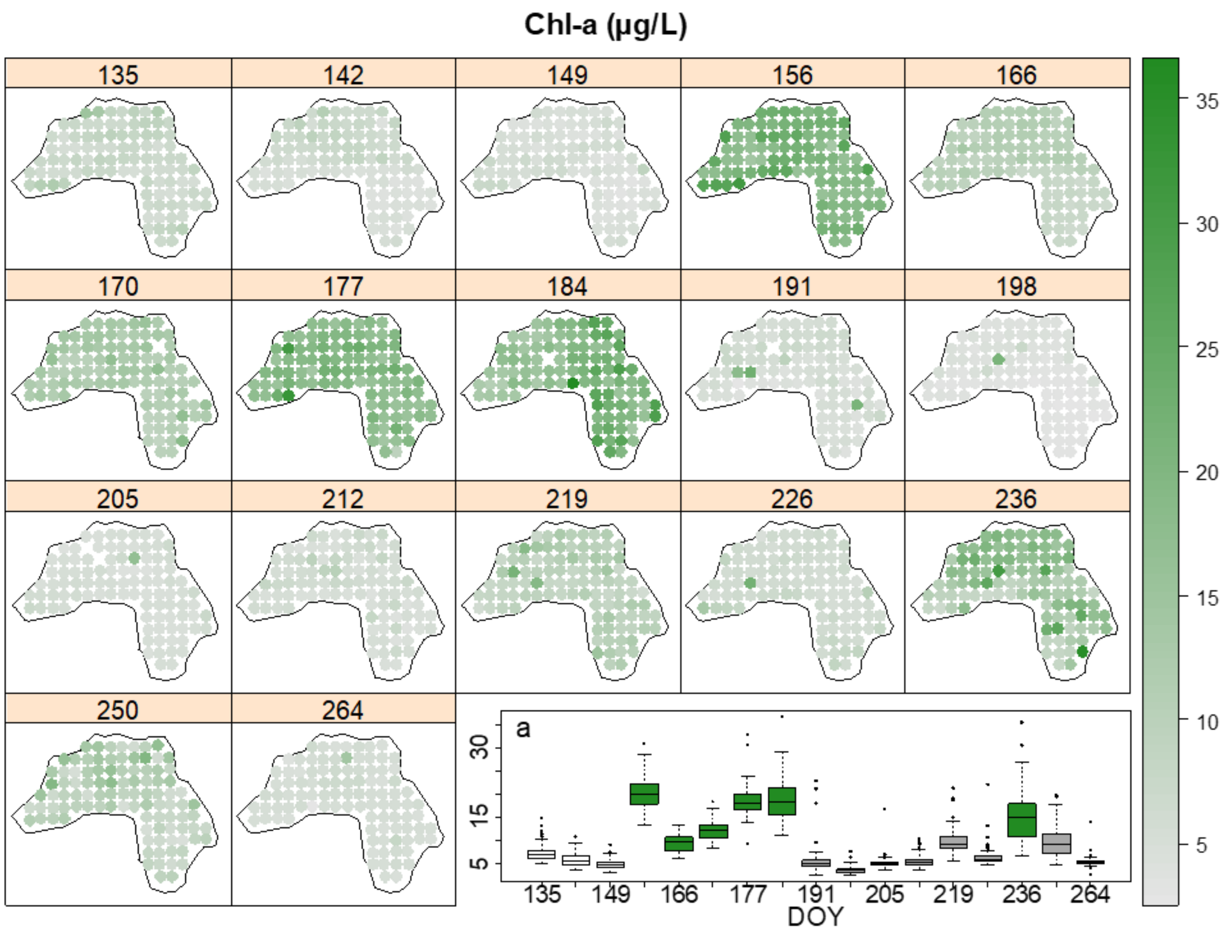

Figure 3.3 Spatial distribution of chlorophyll *a* during 17 sampling events in Swan Lake in 2018. The numbers above each panel outline are DOY and the color ramp on the right side of the plot corresponds to the chlorophyll *a* concentration (µg L^{-1}). Boxplot is the weekly distribution of all values of chlorophyll *a* with the white boxes as the pre-bloom period, green the bloom period, and grey for post bloom (a).

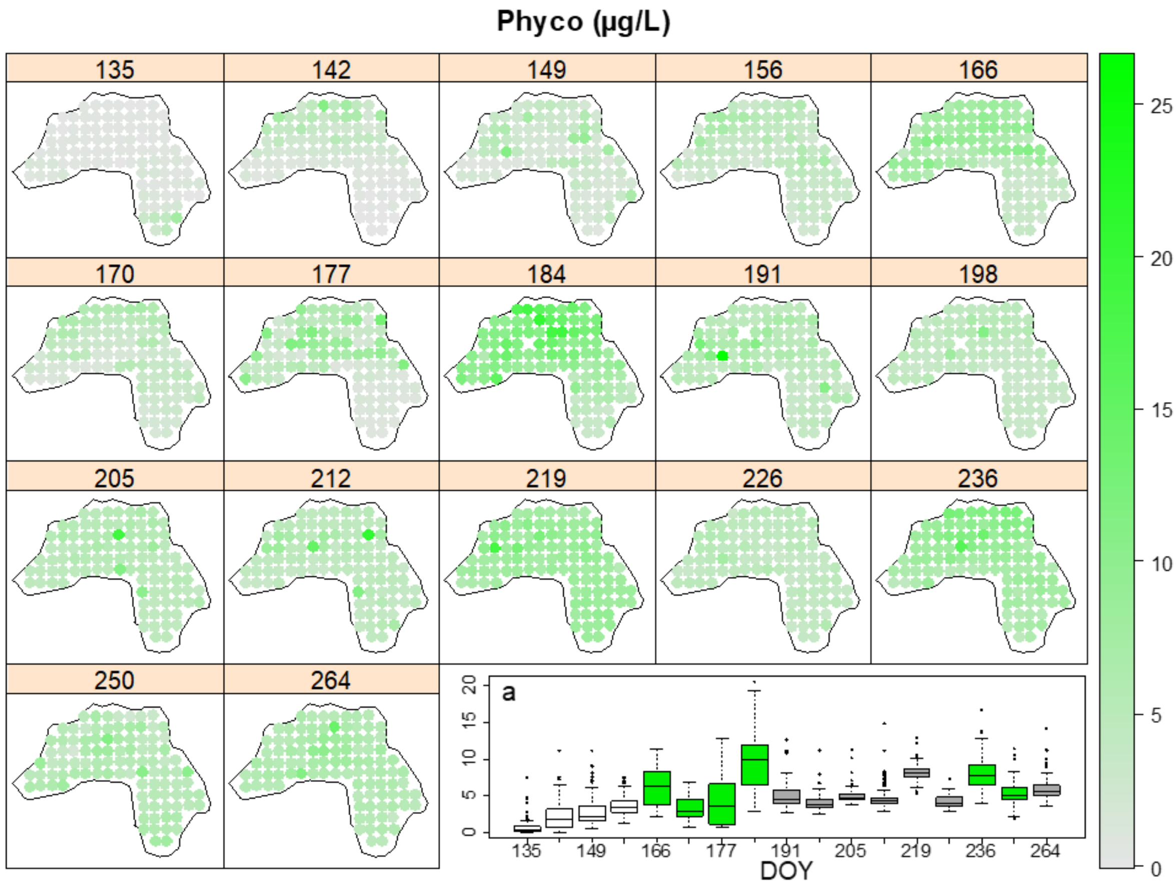

Figure 3.4 Spatial distribution of phycocyanin during 17 sampling events in Swan Lake in 2018. The numbers above each panel outline are DOY and the color ramp on the right side of the plot corresponds to the phycocyanin concentration (µg L-1). Boxplot is the weekly distribution of all values of phycocyanin with the white boxes as the pre-bloom period, green the bloom period, and grey for post bloom (b).

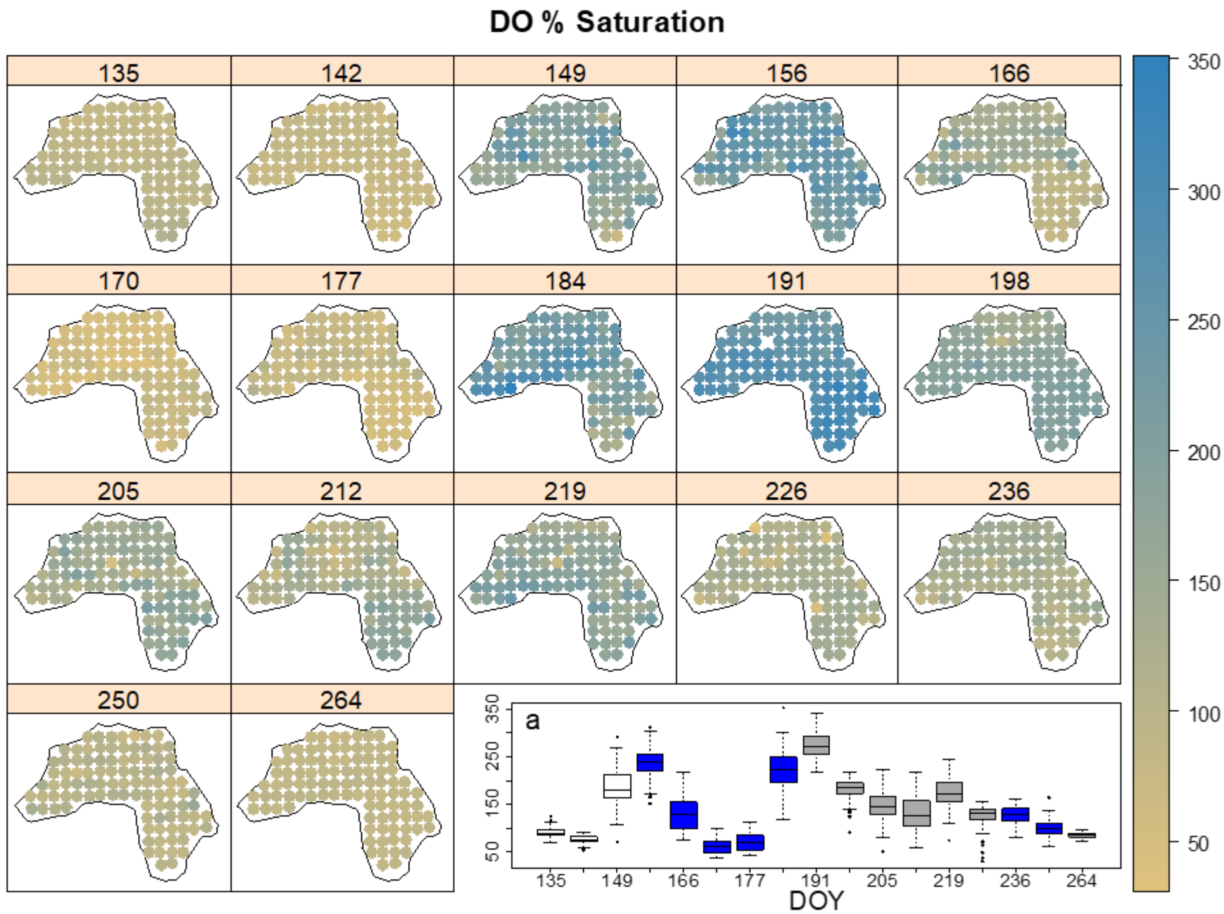

Figure 3.5 Spatial distribution of dissolved oxygen percent saturation during 17 sampling events in Swan Lake in 2018. The numbers above each panel outline are DOY and the color ramp on the right side of the plot corresponds to the DO saturation. Boxplot is the weekly distribution of all values of dissolved oxygen percent saturation with the white boxes as the pre-bloom period, green the bloom period, and grey for post bloom (a).

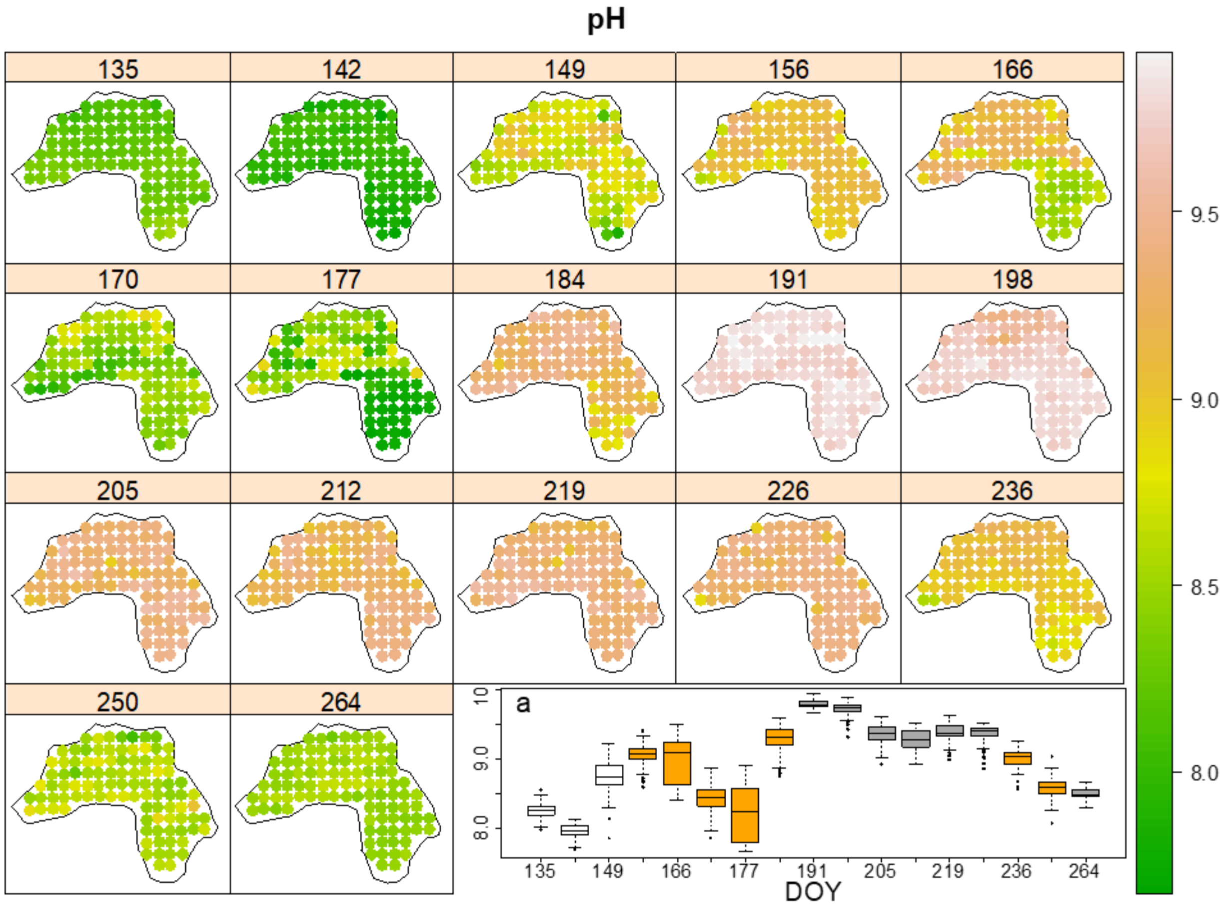

Figure 3.6 Spatial distribution of pH during 17 sampling events in Swan Lake in 2018. The numbers above each panel outline are DOY and the color ramp on the right side of the plot corresponds to the pH. Boxplot is the weekly distribution of all values of pH with the white boxes as the pre-bloom period, green the bloom period, and grey for post bloom (a).

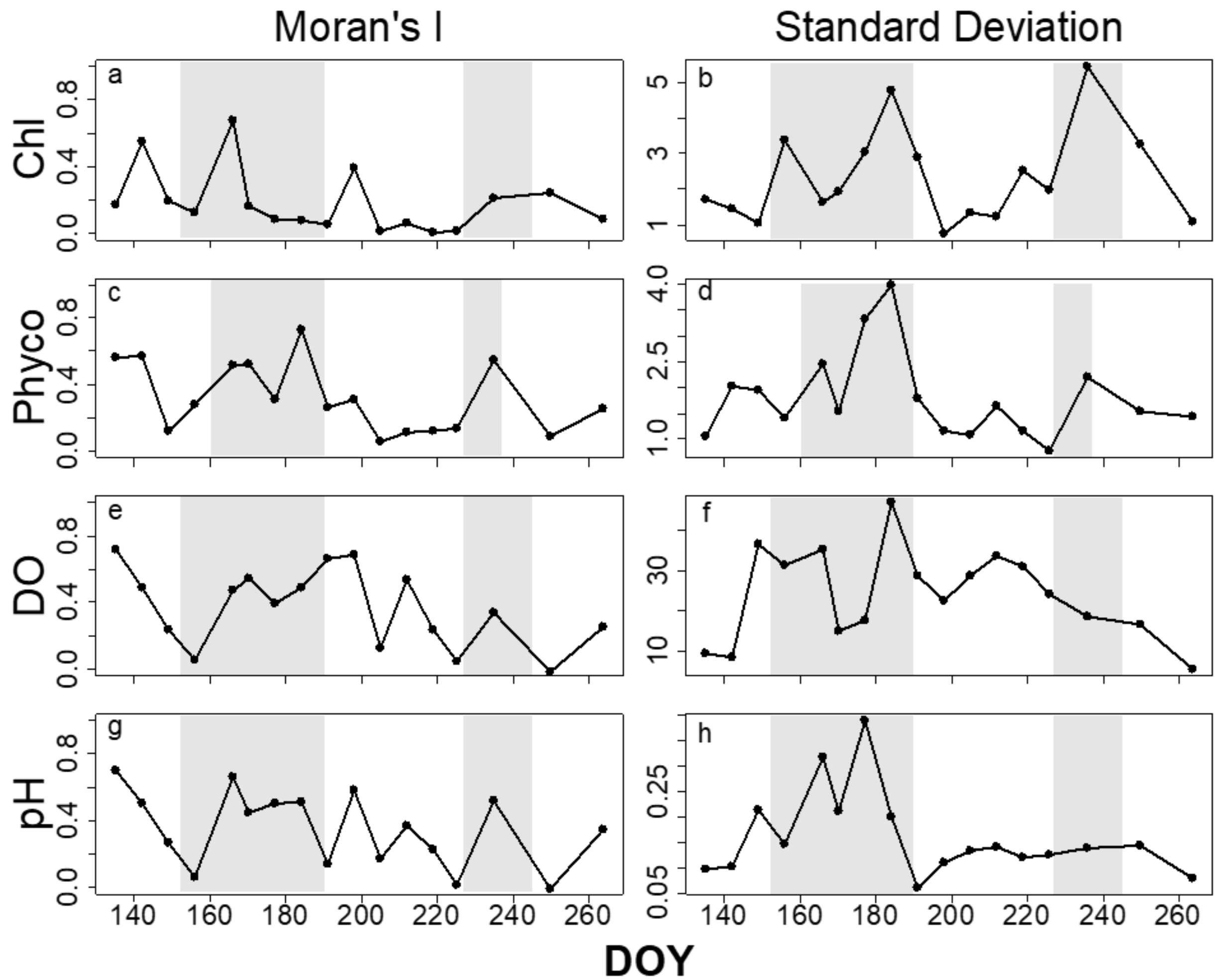

Figure 3.7 Spatial autocorrelation (Moran's I; panels a, c, e, g) and spatial variance (standard deviation; panels b, d, f, h) over the entire study period. Grey areas indicate bloom periods.

CHAPTER 4. GENERAL DISCUSSION

This combined body of work demonstrates the application and possibility of detecting regime shifts in time and space prior to blooms and peak algal biomass in non-experimental hypereutrophic and shallow lakes. We wanted to test the efficacy of temporal monitoring for early warning indicators of impending algal blooms in a variety of non-experimental lakes and test the hypothesis that spatially detecting regime shifts is possible in a non-experimental lake. We detected early warning indicators, rises in state variables summary statistics: standard deviation and autocorrelation, in non-experimental, hypereutrophic, and shallow lakes. This combined body of work contribute to regime shift detection literature and move forward the current state of the field by exploring both time and space monitoring approaches in novel systems.

We were able to detect early warning indicators temporally in all five lake years included in our dataset prior to blooms and algal peak biomass for all state variables. Our five study lakes varied in time monitored, surface area, nutrient loading, shoreline development index values, and depth. In spite of these early warning indicator confounding factors, three of the seven bloom events recorded had a rise in standard deviation or autocorrelation in at least one state variable (chlorophyll *a*, phycocyanin, dissolved oxygen saturation, and pH) prior to the onset of the bloom, warning period lengths averaged two weeks prior to blooms. When considering the apex of the bloom, all five lake years had early warning indicators prior to the peak biomass with a mean warning period of almost four weeks. In addition to detecting temporal rises in summary statistics, we were also able to detect rises in spatial summary statistics by sampling weekly on a coarse 65 m sampling grid in a non-experimental lake. Rises in spatial standard deviation and spatial autocorrelation were interpreted as both early warning indicators and evidence of regime shift detection. When early warning indicators were detected, the warning period averaged 13 days prior to the bloom for all state variables and summary statistics. Detecting rises in summary statistics as evidence of a regime shift, consistently occurred during the first sampling event after the bloom started. As opposed to the temporal monitoring for regime shifts, we found that the unanticipated contribution to net ecosystem production from macrophytes to be major driver of state variables spatial dynamics.

In both instances, time and space, we had to overcome several factors that would inhibit the detection of rising summary statistics, such as stochastic nutrient loading, spatial complexity, and additional sources of net ecosystem production. These studies although successfully able to detect regime shifts and insightful to what future roles temporal and spatial monitoring may serve to lake management, they bring to light several new knowledge gaps of regime shift monitoring. How early do sondes need to be deployed in the ice-off period or do we need to monitor year round? Can high frequency monitoring be enhanced by supplementing with spatial data or can spatial data predict blooms better? Can the number of spatial sample locations and variables monitored be reduced and still detect informative rises in standard deviation and autocorrelation? Is there a scalable relationship between the number of sample locations and lake size? While we were able to begin addressing many of these questions (e.g. the reliability of pH and DO as state variables and the monitoring period needed), these questions need to be further addressed before temporal and spatial early warning detections can be recommended as a tool for lake management.

These studies expand our understanding of regime shifts in lakes, by moving into the realm of testing the efficacy of early warning indicator detection in non-experimental systems using different monitoring methods. Our studies applied theories to lakes under non-experimental conditions and produced results that are in support of previous simulated and experimental conclusions of regime shift detection of both temporal and spatial studies. High frequency monitoring is proving itself an efficient and reliable tool in the effort to understand and manage our heavily impaired waterbodies paired with the empirical evidence that detection of regime shifts spatially is possible, we move forward this field from simulations and experimental lake monitoring to testing the replicability of these observed phenomenon in novel systems.